Characterization of molecular motions in proteins using relaxation data

Akshay Kumar

MS12123

A dissertation submitted for the partial fulfilment of

BS-MS dual degree in Science

Indian Institute of Science Education and Research Mohali

April 2017

Certificate of Examination

This is to certify that the dissertation titled "Characterization of molecular motions in proteins using relaxation data" submitted by Mr. Akshay Kumar (Reg. No. MS12123) for the partial fulfilment of BS-MS dual degree programme of the Institute, has been examined by the thesis committee duly appointed by the Institute. The committee finds the work done by the candidate satisfactory and recommends that the report be accepted.

Prof. Arvind Dr. Samir Kumar Biswas Dr. Kavita Dorai

(Supervisor)

Dated: April 21, 2017

Declaration

The work presented in this dissertation has been carried out by me under the guidance of Dr. Kavita Dorai at the Indian Institute of Science Education and Research Mohali.

This work has not been submitted in part or in full for a degree, a diploma, or a fellowship to any other university or institute. Whenever contributions of others are involved, every effort is made to indicate this clearly, with due acknowledgement of collaborative research and discussions. This thesis is a bonafide record of original work done by me and all sources listed within have been detailed in the bibliography.

Akshay Kumar

(Candidate)

Dated: April 21, 2017

In my capacity as the supervisor of the candidates project work, I certify that the above statements by the candidate are true to the best of my knowledge.

Dr.Kavita Dorai

(Supervisor)

Acknowledgements

First and foremost I would like to express my deepest gratitude to my advisor Dr. Kavita Dorai. This project would not have been possible without the guidance and support provided by him. I would like to thank my thesis committee, Dr. Kavita Dorai (Supervisor) , Prof. Arvind and Dr. Samir Kumar Biswas for taking out the time to read my thesis and giving valuable suggestions. I am extremely thankful to Prof. N. Sathyamurthy, Director, IISER Mohali, for allowing me to use the various facilities of this institute to carry out the research work. I would also like to thank IISER Mohali for giving me this wonderful opportunity, first to study in a research oriented environment and then allowing me to do the final year research. The scientific discussions with the faculties and students over these years have opened my mind to the existence of different possibilities in the ever changing field of Science. I would also like to thank Department of Science and Technology (DST) for providing me INSPIRE Scholarship for Higher Education (SHE).

I would also like to thank Rakesh Sharma for helpful discussion. At last, I would like to thank my friends Nitesh Kumawat,Sanjib Kumar Das, Abhijeet Roy, Vikram Singh Bhati,Shrinit Singh, Prem Kumar, Mukesh, Rahul, Ashish, Gaurav Saxena and my all NMR lab members for being always with me. It was due to their constant support that I did not feel lost at any time.I also would like to convey my special thanks to Dr. Sachin Chaudhary for his guidance. I would like to acknowledge the respect that I got from junior batches and the love given by the seniors. I am taking a lot from here and hope that I will be able to do justice to the support and guidance provided by IISER Mohali.

Aksahy Kumar

IISER MOHALI

Dedicated to my family and friends

For their endless love,support and encouragement

Contents

Bibliography

List of Figures

Abstract

Structures alone cannot explain protein functions and biochemical data. Studying dynamics on different timescales play an important role in understanding protein functions. NMR relaxation experiments provides wealth of information about molecular dynamics in macromolecules and fluids.To get the meaningful explanation of NMR relaxation data, Model free approach for analysis of the data is used.We analyse the spin-relaxation experimental data(R_1, R_2, NOE) within the model free formalism (Clore et al.1990; Lipari and Sizabo,1982)to study and analyse molecular dynamics with atomic resolution of biomolecules like Ubiquitin, RNase and 14-mer RNA using the program FAST-Model free for the fully automated, high throughout analysis of NMR spin relaxation data.

Chapter 1

Introduction

Since the discovery of magnetic resonance in mid- 20th century, nuclear magnetic resonance has become a powerful interdisciplinary method where we can work on the interface of physics, chemistry and biology to study biomolecules and the materials. Since mid- century as many as nine nobel prize has been awarded in magnetic resonance. Some important names in the history of Magnetic resonance who got nobel prize starting from first in 1944 till today are *Isador I. Rabi* in 1944, *Felix Bloch* and *Edward M. Purcell* in 1946, *Richard Ernst*, *Kurt Wthrich*, *Paul C. Lauterbur* and *Sir Peter Mansfield* for their pioneering contributions to enabling the use of magnetic resonance in medical imaging in 2003. As we know superconducting materials have very important role in magnetic resonance, *Alexeij A. Abrikosow* and *Vitalij L. Ginzburg* received noble price in 2003 for significant contribution in superconductors theory.

1.1 Introduction to NMR Spectroscopy

NMR stands for Nuclear magnetic resonance. It is also a spectroscopic technique like Ultra-violet, Infrared and Raman spectroscopy. The very basic of the NMR experiment is that we apply a radio-frequency pulse to a sample and observe how the sample behave by taking a Free Induction decay(FID) which is further Fourier transform to give spectrum (in frequency domain).

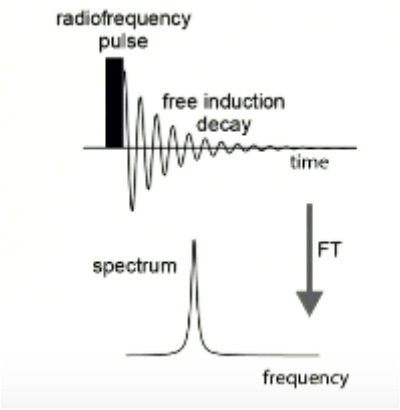

Figure 1.1: Fourier transform of FID into spectrum[31].

The magnetisation is excited and observed and the time domain signal is transformed into the frequency domain by Fourier transformation into spectrum. We can measure the return of magnetisation after being excited which includes longitudinal relaxation and transverse relaxation.

There are many other experiments like COSY, HSQC, and INEPT but we will stick to only T_1, T_2 and NOE in our analysis of proteins using model free analysis.

When the sample is placed inside the NMR spectrometer it experience central high magnetic field. The sample is surrounded by different RF coils which are used to send the RF pulse for the experimental analysis of the sample. It turnout that the sample which is within the coil range contribute to the signal. The rest of the sample in the bottom of the tube does not significantly contribute to the signal. The central

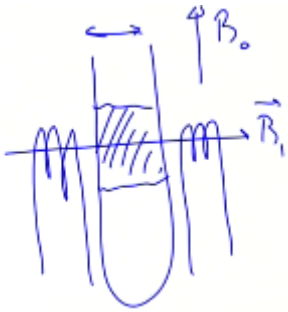

Figure 1.2: schematic representation of sample between RF coils with B_0 is central field and B_1 is RF magnetic field.

magnetic field B_0 which we are talking about is high and sharp but it turns out that this magnetic field is actually not homogeneous through the sample rather the line of flux goes slightly stretched. If we consider two volume elements V2 and V1, as a

result of this homogeneity V1 experience more uniform intense magnetic field then V2 and the other which are at the edges of the tube.

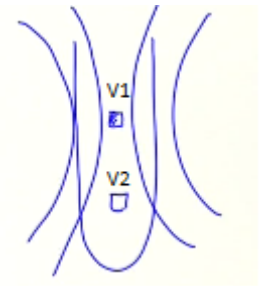

Figure 1.3: Representation of the inhomogeneity of magnetic field in sample among volume elements V1 and V2.

So the V1 box gives rise to higher frequency than the V2 in the observed signal. Since we have many of these kind of volume elements at different positions in the sample so the resultant gives rise to somewhat broader peak with half width D.

$$D = \frac{1}{\pi {T_2}^*} \; ; \; d = \frac{1}{\pi T_2}$$

Where D is the apparent half width which appear to us in the signal and is related

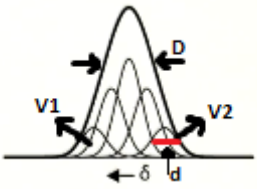

Figure 1.4: peak broadening d in elements V1 and V2 and also the resultant broadening D due to inhomogeneity in magnetic field.

to apparent relaxation time ${T_2}^*$. While d here is the actual half width of the elements which is related to actual transverse relaxation time T_2.

1.1.1 Vector model

$$M = \begin{bmatrix} Mx \\ My \\ Mz \end{bmatrix}$$

Magnetisation has three components.

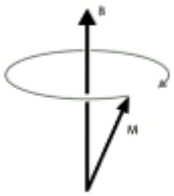

Figure 1.5: resultant magnetisation vector precessing around central magnetic field with larmer frequency[32].

So, for the case if we have only z- component of magnetisation and other components are zero then this magnetisation vector aligns with the magnetic field and nothing is going to happen. So, magnetisation to precess we need to make its transverse component non- zero. Now let if it has transverse component, it starts to precess around the static magnetic field. The frequency of this precession is known as *Larmer frequency*. This frequency basically turn out to be equal to energy difference between the two states.

$$\omega_o = \frac{\Delta E}{\hbar},$$

where ΔE is the enery difference between the two states α and β of the measured nucleus.

Effect of RF pulse

We are working in the rotating frame and adjusted static B_1 (RF magnetic field) in x-axis. Now, applying RF pulse in x-direction flip the z-magnetisation into negative y-axis which when left for some delay time τ develops the phase in x-y plane.

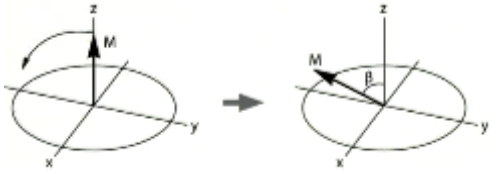

Figure 1.6: magnetisation flip due to application of RF pulse[32].

$$\beta = \gamma B_1 \tau_p,$$

where β is the flip angle, γ is gyromagnetic ratio of the nucleus, τ_p is flip duration and B_1 is the RF magnetic field.

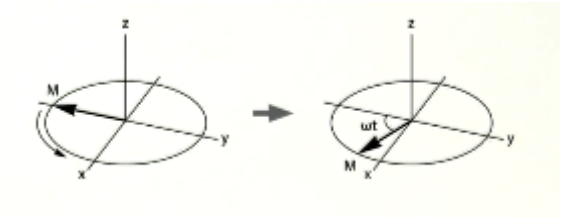

Figure 1.7: building of phase in X-Y plane[32].

$$\phi = \omega t$$

$\omega = \omega_o \omega_{rot}$, where ω_o is true frequency and ω_{rot} is frequency of rotating frame.

Free Induction decay

When we apply a RF pulse and observe the free induction decay of the magnetisation in transverse plane it gives us FID in time domain. To get a spectrum we need to convert it into frequency domain. That is basically done by Fourier transformation of time domain signal into frequency domain. The above is the example of the Fourier

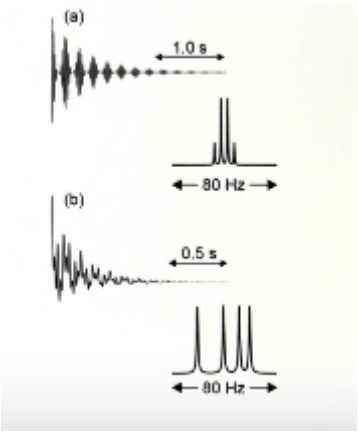

Figure 1.8: Free Induction decay to spectra for different nuclei[32].

transformation from a FID to spectra. In (a) the FID gives rise to a signal showing a Quadrat after the Fourier transformation of FID while in (b) there are four different peaks observed after the Fourier transformation.

Now after getting the spectra we can use the signal averaging to reduce noise and get high intensity of the peaks. The main advantage of signal averaging is that the intensity level increases linearly with the number of scans where noise increases as square root of number of scans.

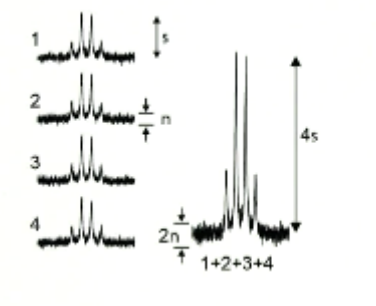

Figure 1.9: intensity integration to enhance sensitivity by increasing number of scans along with noise.Signal S goes as 4S, while Noise n goes as $\sqrt{4 * n} = 2n$[32].

1.1.2 Advantages of Molecular dynamics study

Since past decade there are large number of structures of proteins using x-ray crystallography and the multidimensional NMR has been identified. Knowing the structure help us understanding things like co-ordinate information about each residue in the protein and much more. But structure alone cannot explain the functions of protein. Since many functions of the protein depends upon the conformational dynamics of the protein. So it is very important to understand the dynamics of the protein to understand the protein fully.

For example, how a ligand access the active site of an enzyme may require conformational rearrangements. Enzyme catalysis and ligand off-rates have been measured to be on the order of $1010^5 s^{-1}$ and folding rates for small globular proteins are in the range of $10^{-1}10^5 s^{-1}$ [4].

But not only the slow internal motions are of importance to understand the protein fully, Fast internal motions plays a very crucial role because the fast motions on time scale of piconano second are associated with the entropy which allow us to know the number of states that are available to specific sites of the protein. So it acts as entropy estimation meter. Changes in the functional states are often associated with redistribution of this entropy[3].

1.1.3 Why we use NMR?

The main question which pop up in our mind is why we use NMR? The answer to this question is very simple, it is because NMR experiments provides us wealth of

information on protein architecture. NMR spectroscopy has been successfully used to measure protein folding rates[54, 55] and for direct observation of protein-ligand interaction kinetics[54]. Furthermore, the insights heteronuclear NMR relaxation measurements can provide on the role of protein motions in molecular recognition have been reviewed[2].

The advantage of NMR compare to the other spectroscopy technique like X-ray crystallography which is also used to study the structure of proteins is that it does not free the protein sample in time unlike the x-ray crystallography so all the dynamics of the proteins are available to us for study. The main advantage of the NMR is that here we can probe the molecular motions with atomic resolution. So NMR turn out to be good method to understand the proteins fully.

1.1.4 What Information does NMR relaxations provide?

As we have pointed out earlier also that the motions faster than the overall tumbling influences the relaxation parameter by influencing the dipole-dipole and Chemical Shift Anisotropy hamiltonians. Fast internal motions can be probed by laboratory frame relaxation measurements of spins whose relaxation mechanisms are associated with a bond vector. The data are most commonly analysed using the model-free approach introduced by Lipari and Szabo[1] with some restrictions for model fitting. NMR relaxation parameters are sensitive to rotation of these bond vectors around a perpendicular axis. These fast internal motions are related to entropy of the protein and hence gives us idea about the flexibility of the protein. For model-free analysis N^{15} is probed for backbone motion with N-H as bond vector under consideration. Because this has become a virtual routine and most of the other program do the same. For the study of side chain motion in proteins C^{13} labeled CH_n groups can be converted into CHD_{n-1} moieties via deuteration and C-H bond vector can be used for the analysis[1, 2, 4].

Chapter 2

Internal motions

2.1 Spin-$\frac{1}{2}$ Nuclei

As we are dealing with liquid NMR spectroscopy, proteins can possess multiple degree of freedom and hence have different types of motions which motivates us to study the dynamics of the protein. Because most of the interactions of the molecules can be understand by understanding these different time scale motions. we characterise these motions into two category:

1.Fast Internal Motions

2.Slow Internal Motions. Many functions of the biological molecules or systems are

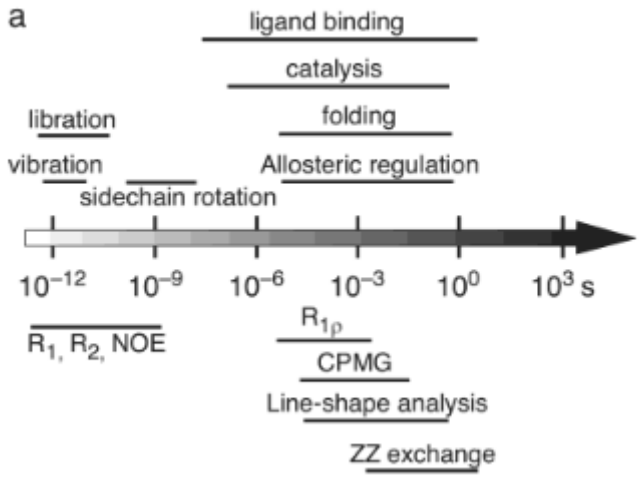

Figure 2.1: time scale motion dependence in protein[52].

directly related to spatial and temporal changes in it. The very essence of many

biological process rely on transfer of information through conformational exchange associated with protein folding, ligand binding, chemical exchange etc.
In fig.2.1 we can understand the different time scale motions study of the proteins or any other biomolecule gives us wider knowledge of the different interactions arise due to the phenomena like the vibrations, liberations, ligand binding, protein folding etc.

2.1.1 Fast Internal Motions

we have a protein in which we want to understand the different functions of that protein with different time scales using liquid state NMR. So in the sample the protein is allowed to do Brownian motion which is the overall tumbling of the molecule and can be related to the overall correlation time for the protein. The overall rotational correlation time can be derived by the stocks law. The rotational correlation time here is defined as the time it taken by a molecule to rotate by one degree. More is the size of the molecule, higher is the rotational correlation time. The motions which are faster than the overall tumbling of the protein are considered as the Fast internal Motions. The time scale fast motions ranges from nano-second to pico-second which are basically vibrations, liberations and side chain motions mainly. These fast motions affects the relaxation parameters also and hence can be related to relaxation parameters and the correlation functions.
The overall rotational correlation time of the globular protein with a spherical approximation (isotropic diffusion) which is the characteristic of Brownian diffusion in a liquid can be derived by Stokes law[63] as:

$$\tau_c = 4\pi\eta_w \frac{{r_H}^3}{3K_B T}$$

Where τ_c is the overall rotational correlation time of the molecule ,η_w is the viscocity of the liquid, r_H is the hydrodynamic radius which is related to the molecular weight of the protein, k_B is the Boltzmann constant and the T is the temperature of the system. The hydration radius can be calculated as [63, 62]:

$$r_H = [3\bar{V}M_r/4\pi N_A]^{1/3} + r_w$$

Where V is the specific volume (cm^3/g) of the protein,M_r is the molecular mass of the protein, N_A is the usual avogadro number and the r_w is the hydration radius which is

usually between 1.6 Åto 3.2 Å(which is one half of one hydration shell). The general thumb rule to calculate the approximate hydration radius is that it is approximately 0.6 times the molecular weight of the protein in KDa. Above discuss method was the

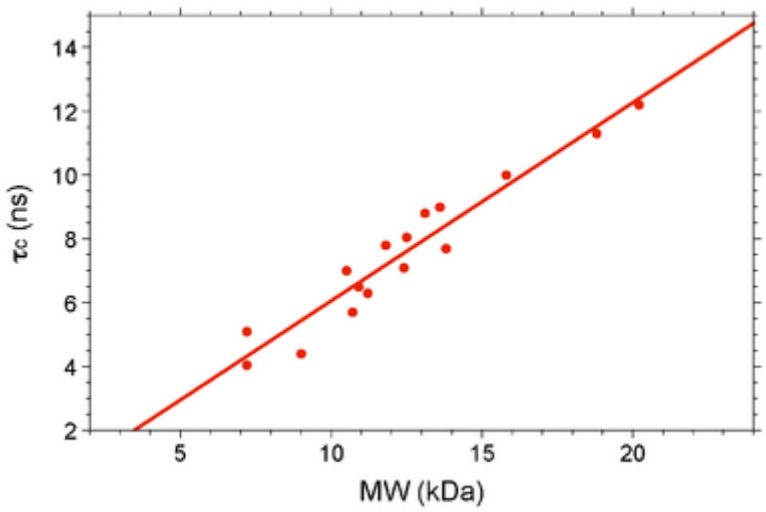

Figure 2.2: An example of correlation time vs Molecular weight of proteins in kDa[63].

method to calculate rotational correlation time by hydrodynamic calculations. But as we have shown above that the rotational correlation time can also be calculated by relaxation parameters. For rigid protein molecules, in the limit of slow molecular motion ($\tau_c >> 0.5ns$) and high magnetic field (500 MHz or greater), a closed-form solution for τ_c as a function of the ratio of the longitudinal (T_1) and transverse (T_2) N^{15} relaxation times exists[63, 61]

$$\tau_c \approx \frac{1}{4\pi\nu_N}\sqrt{6\frac{T_1}{T_2} - 7},$$

Where, ν_N is the N^{15} resonance frequency (in Hz) ,T_1 is the longitudinal relaxation time, T_2 is the transverse relaxation time. The validation of the above relation to give a real rotational correlation time rely on the fact that the $T_1 > T_2$ such that $6T_1/T_27 > 0$, which is true in case of almost all proteins with no difficulty. Below is a table of rotational correlation time values compiled for known monomeric NESG targets[57]. All data was recorded on a Bruker 600 NMR instrument at 298 K. The molecular weight for each target takes into account isotopic enrichment and the presence of affinity purification tags.

NESG target (isotope labeling)	MW (kDa)	^{15}N T_1 (ms)	^{15}N T_2 (ms)	τ_c (ns)
PsR76A (NC5)	7.2	478.0	128.0	5.10
VfR117 (NC)	11.2	605.0	119.0	6.30
SyR11 (NC5)	12.4	630.0	104.0	7.10
ER541-37-162 (NC5)	15.8	729.0	66.5	10.0
ER540 (NC5)	18.8	909.0	66.5	11.3
SoR190 (NC)	13.8	697.5	100.9	7.70
TR80 (NC5)	10.5	612.8	102.9	7.00
Ubiquitin (NC)	9.0	441.8	144.6	4.40
HR2873B (NC)	10.7	492.0	115.0	5.70
B-domain (NC)	7.2	423.5	153.3	4.05
BcR97A (NC)	13.1	705.8	80.6	8.80
PfR193A (NC)	13.6	733.9	80.9	9.00
MvR76 (NC)	20.2	1015.0	64.5	12.2
DvR115G (NC)	10.9	608.7	115.6	6.50
MrR110B (NC5)	11.8	707.0	99.2	7.80
VpR247 (NC5)	12.5	661.2	88.3	8.05
BcR147A (NC)	11.9	645.0	104.0	7.20
WR73 (NC5)	21.9	1261.0 *	41.3 *	13.0
NsR431C (NC5)	16.8	855.5	71.2	10.6
StR82 (NC)	9.2	537.3	100.4	6.6

Figure 2.3: Table of rotational correlation time values compiled for known monomeric NESG targets[57, 63].

2.1.2 Slow internal motions

As discussed earlier the internal motions in protein can vary in time scales, the motions which are on time scale slower than the molecular tumbling of the protein are considered as the slow internal motions. The time scale of these motion ranges from microseconds to seconds. The study of protein folding, chemical exchange rate, ligand binding etc comes under the study of slow internal motion. Chemical exchange rate[20] are very important and provide us information about orientations and chemical kinetic processes. The main experiments to get chemical exchange are longitudinal magnetisation exchange, line shape analysis, CPMG and R_1 row relaxation exchange[20]. But we are not going to discuss more about the study of slow motions rather than we will focus on the fast internal motions which can be studied using our relaxation parameters in model free analysis. This is due to the reason that conformational dynamics which is going on the scale faster than the overall correlation time or equal to overall correlation time influence the relaxation mechanism dipole-dipole, CSA Hamiltonians. The key thing to remember is that in most of the protein application N^{15} amide group is considered as probe to backbone motions and the N-H bond vector is the main centre of attraction for the backbone motions while the proton in C-H bond vector in methyl group is probed as side chain motion of the protein[29, 30].

2.1.3 R_1 and R_2 Relaxation

R_1 and R_2 are basically the relaxation rates which are only the inverse of relaxation times T_1 and T_2 respectively.

Relaxation times in a very simple sense tells us how the magnetisation return to equilibrium after being disturb from equilibrium by application of a RF pulse. Here we refer equilibrium as the population distribution in levels (ground and the excited) as predicted by Boltzmann distribution and the magnetisation is directly proportional to population difference between these levels. The alternate explanation in term of states of a nuclei can be given as the return of population from excited state to ground state. Relaxation in NMR is a slow process as compare to other spectroscopic techniques for example in where relaxation in vibrational and electronic transition of time scale pico- second to microsecond is concerned. The NMR relaxation times are order of the few seconds commonly (0.1 Sec to 100 sec) which allow us to saturate NMR transitions i.e. we can equally populate the excited and the ground state.

There are two types of relaxation of magnetisation which we measure by different experiments using different RF pulse sequence.

1. Longitudinal Relaxation time.
2. Transverse relaxation time.

Longitudinal Relaxation time(T_1)

Longitudinal relaxation is the measure of the return of the Z-magnetisation back to the equilibrium after being disturb from the equilibrium position. It is also known as spin lattice relaxation or relaxation in Z-direction. The longitudinal relaxation time (T_1) is measure by the most common inversion recovery experiment. The pulse sequence of the inversion recovery experiment is given in fig.2.4.

In this experiment we start with the initial z-magnetisation, A 180° pulse is applied first which invert the net z-magnetisation into the negative z-magnetisation followed by a delay time τ which allow the magnetisation to evolve with the time. Then we apply a 90° pulse to get magnetisation in x-y plane and we can record the FID which can be further Fourier transform to get spectrum.

The experiment is repeated with different delay times usually for five different delay

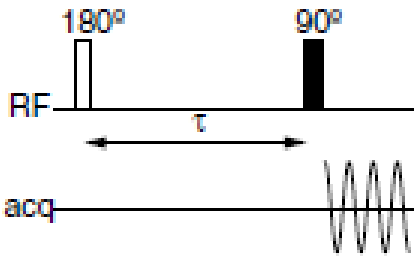

Figure 2.4: Inversion Recovery pulse sequence[32].

times to check the behaviour of magnetisation for different time intervals. There are

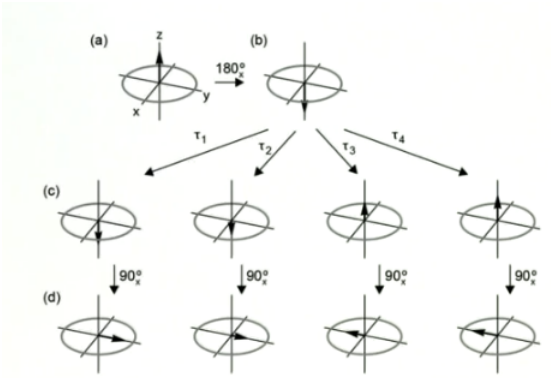

Figure 2.5: Schematic of how the magnetisation recovers with different delay times in inversion recovery experiment[32].

four different times are shown in this figure above. The fifth delay time which we refer to is the delay time in which the z-magnetisation turns its sign and start returning to positive z-direction.

As we can see when we apply a 180° pulse the z-magnetisation flips its sign and gives a net z-magnetisation in $-ve$ z-direction. The magnetisation starts recovering and the amplitude in $-ve$ z-direction starts to decrease with time and finally recovers to its equilibrium z-direction of magnetisation. We record the signals at given time delays as described in the above diagram and plot magnetisation vs time to see the recovery behaviour of the magnetisation[32, 31].

$$S(\tau) = [1 - 2exp(-\tau/T_1)]S(\infty)$$

Where, $S(\tau)$ is the signal intensity measured, τ is the delay time (as τ_1, τ_2, τ_3 and τ_4

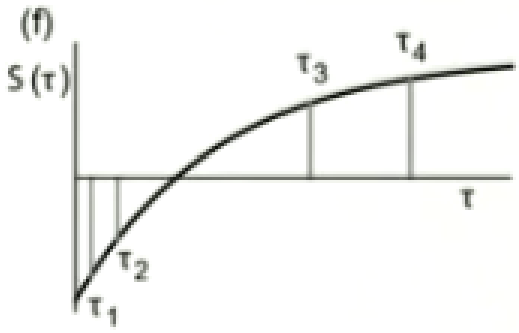

Figure 2.6: Intensity vs time graph showing exponential dependence of magnetisation on relaxation time (T_1) [32].

are used in example) and T_1 is the longitudinal relaxation time.

Now, the significance of knowing the longitudinal time is that it gives you information about the environment of nuclei. That is how fast a nuclei relaxes is depends on its environment. We will try to see this by an example here. Let us take the example of 1,3- di-nitrobenzene and we want to see how the different hydrogen or say protons relaxes with time. H2, H4, H5 and H6 represents the hydrogen present at 2,4,5,6 positions of 1,3-dinitrobenzene respectively.

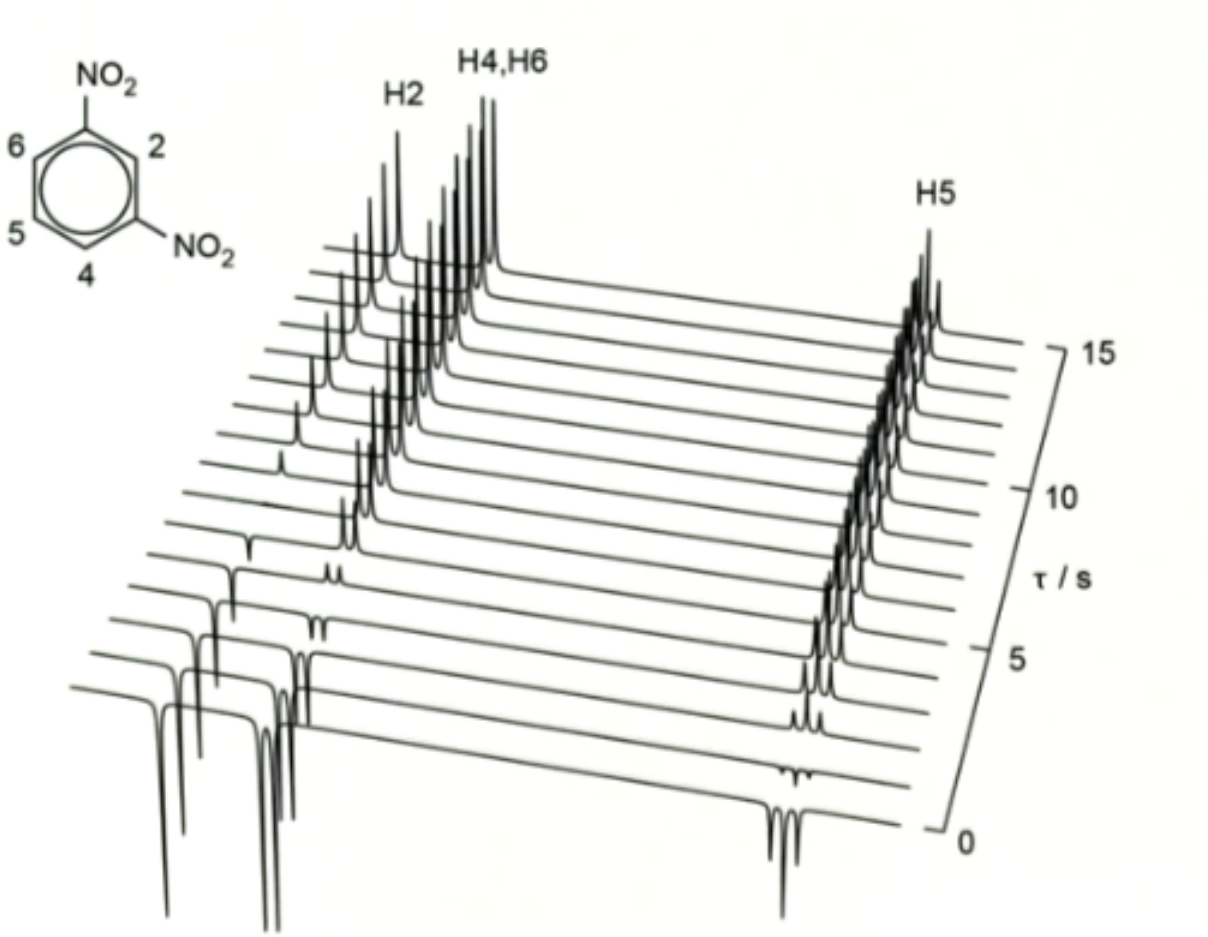

Figure 2.7: Relaxation times of different Hydrogens in 1,3-di-nitrobenzene[32].

This is a really nice example which tells us that how the interaction from neighbour nuclei directly affect the longitudinal relaxation of magnetisation since the magnetisation is directly proportional to the signal intensity we get in the spectrum we analyse it directly from peak heights.

In the above example, H5 relaxes most rapidly that is magnetization get recovered to the equilibrium z-direction in very short duration in about 5 seconds duration. While other hydrogens take much longer time as compare to this in recovery of the magnetization.

The main reason of fastest relaxation of H5 is that it experience high dipolar coupling from both neighbour hydrogens which help it to recover faster while H4 and H6 have identical environment and experience dipolar coupling with a single H5 only. But H4 and H6 relaxes faster than the H2 which do not have any neighbouring dipolar coupling with hydrogen due to absence of neighbouring hydrogen that's why H2 takes

much longer time to recover its magnetisation and has longest longitudinal relaxation time among all the hydrogens in 1,3-di-nitrobenzene.

Transverse relaxation time(T_2)

It is the measure of relaxation of transverse component of magnetic field. It is also known as spin-spin relaxation time. The main cause of the transverse relaxation is the decoherence. Decoherence arise due to inhomogeneity of the magnetic field as a result of which the spins which experience higher magnetic fields moves faster than compare to others who experience relative less magnetic field and as a results losses coherence and start to disperse in x-y plane. Since each of the spins experiences different magnetic field so as have different larmer frequency which result in dephasing of the spins in x-y plane.

Relaxation time T_2 is the measure of how magnetisation in transverse plane decays with the time. Basically it is the measure of how much time the transverse magnetisation takes to decay 37% of initial value. The transverse relaxation time is also known as spin-spin relaxation time, it is due to reason that exchange of energy takes place with the neighbouring nuclei having identical precession

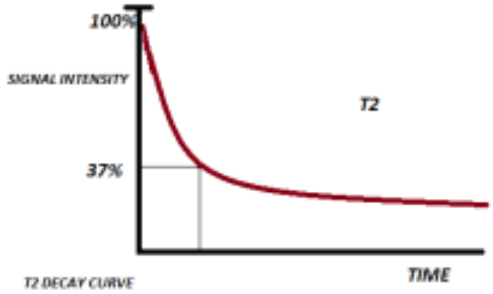

Figure 2.8: Intensity vs time graph for relaxation time(T_2)[66].

frequency but different magnetic quantum states. It can be realised as redistribution among available energy states.

The lower value of T_2 essentially gives us idea that the probability of the energy exchange among the states available by spin-spin relaxation is very low that relative accessibility among the spins is low. For example in fluid where there is large amount of diffusion and spins do not interact much rapidly the T_2 relaxation is low. While the tissue where the spins are much packed in a matrix or highly bonded gives the

faster T_2 relaxation.

The Experiment which is usually perform to measure the transverse relaxation is known as spin- echo experiment. The pulse sequence for this experiment is given as: Instead of applying 180° pulse first (as we do in inversion recovery experiment)

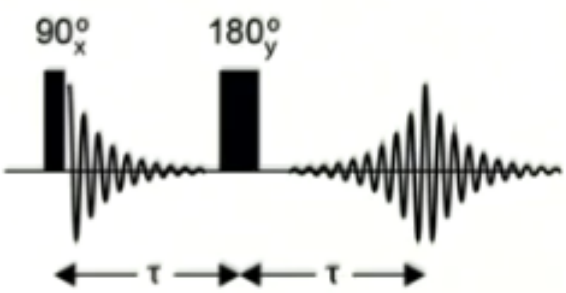

Figure 2.9: Pulse sequence for spin-echo experiment for measuring relaxation(T_2)[32].

we apply a 90° pulse to create the transverse magnetisation. The magnetisation in the x-y plane starts to decay with the delay time τ and we have the usual FID due to delay time. But we apply a other 180° pulse to refocus the magnetisation vector which in the end form an echo that can be recorded.

For further explanation let us look at the vector model of the spin-echo experiment[65, 45].

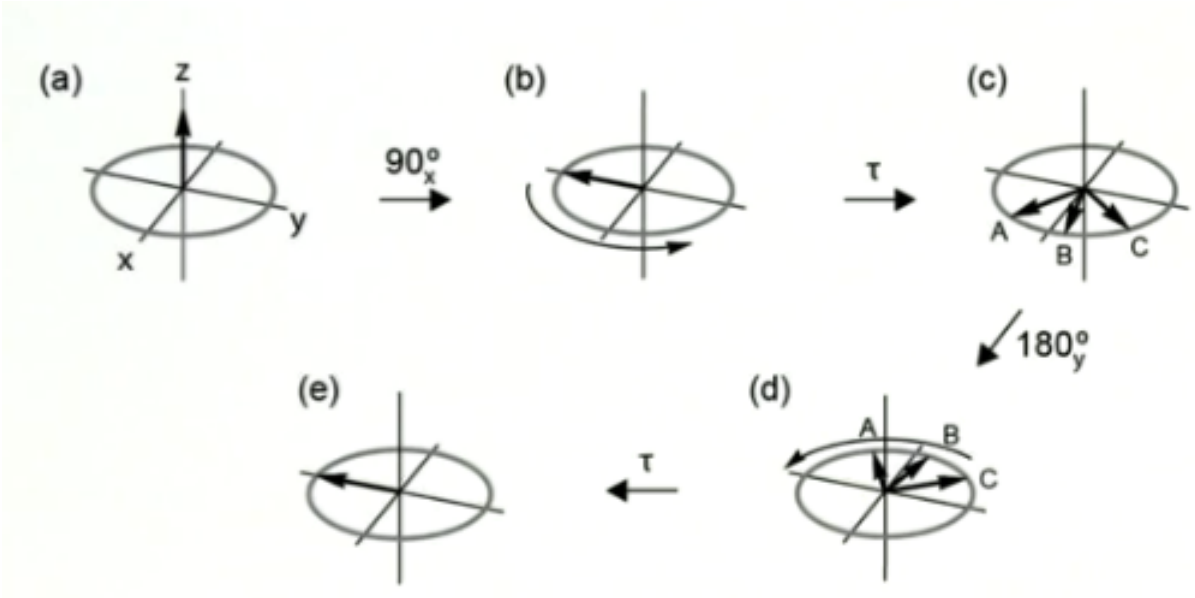

Figure 2.10: Vector model for spin-echo experiment[32].

As shown above, we start with initial z-magnetisation which after application of a

90° x- pulse flips the net magnetisation into y-axis. The magnetisation vectors starts dephasing due to inhomogeneity of the magnetic field. The magnetisation vector A, B, C in this example moves with different speeds due to difference in Larmer frequency. The one who experience high magnetic field possess the highest Larmer frequency as a result moves faster like C as compare to A. now the 180° y-pulse flips all the magnetisation vectors which are dephasing. Now the result of this 180° pulse is that it refocus the magnetisation. The magnetisation vector which was initially moving faster covers has to cover more distance as compare to the others who were slower after the application of 180° pulse. As a result all the vector recovers at the same time and re-established the coherence. The time of dephasing is same as time of rephrasing. Here, In this figure the phase ($\phi = \omega\tau$) for A,B,C for both the delays are

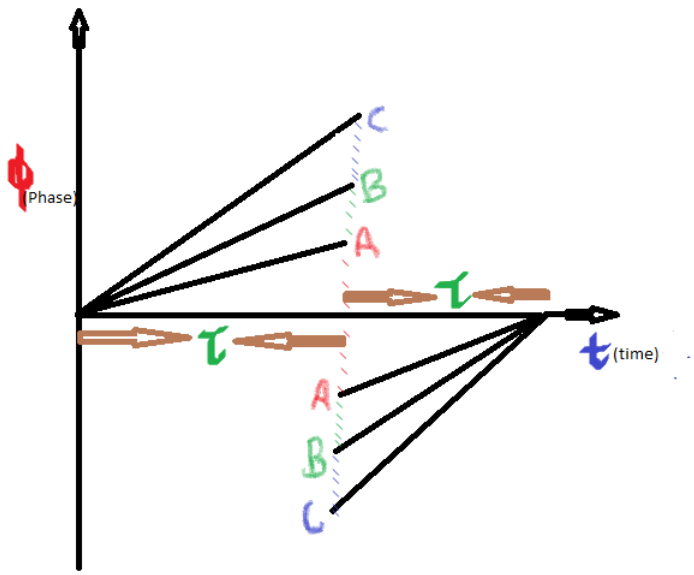

Figure 2.11: Phase vs time graph representing dephrasing and rephrasing that is formation of spin-echo.

shown which tells us that the dephasing and the rephasing times are same.

2.1.4 Heteronuclear NOE

The Nuclear Overhauser Effect is the transfer of nuclear spin polarization from one spin bath to another spin bath via cross-relaxation.It depends on the spatial distance

between the two atoms.It shows a change in intensity of one resonance when the transitions of another are perturbed.The polarization we are talking about here is directly related to the population difference and it depends upon gyromagnetic ratio, magnetic field and the temperature. For example if the two hydrogen nuclei are close by in space then there is possibility of polarisation transfer. So in principle it help us in finding which two protons are close in space.

Let us take the example of Chloro-propane to understand the overhouser effect more deeply. Initially the system of spins till there is no RF applied follow the usual Maxwell Boltzmann distribution. But as we apply a RF pulse on the proton of first nuclei it disturbs the equilibrium distribution. The irradiating RF pulse changes the population distribution on the aimed nuclei and gives rise to a saturation condition. We should remember that spin nuclei which we are talking about here carries magnetic moment and behave as magnetic dipoles. So creation of zero polarisation affect the neighbouring proton if they are dipolar coupled. So as the net result polarization of one spin is disturbed if we apply a RF pulse on its neighbour to which it is dipolar coupled.The NOE can be seen among the nuclei which are 4-5$\mathring{A}$ apart. Nuclear Overhauser Effect SpectroscopY (NOESY)[45] is a 2-Dimension spectroscopy by which we can identify spins undergoing cross-relaxation and can measure the cross-relaxation rates. Most commonly, NOESY is used as a homonuclear proton technique. In NOESY, dipolar couplings provide the primary means of cross-relaxation, and so spins undergoing cross-relaxation are those which are close to one another in space. Thus, the cross peaks of a NOESY spectrum indicate which protons are close to which other protons in space. This can be distinguished from Correlation SpectroscopY(COSY)[45, 65], for example, which relies on J-coupling to provide spin-spin correlation, and whose cross peaks indicate which protons are close to which other protons through the bonds of the molecule.

In NOE, change in population of one proton (or other nucleus) is done when another magnetic nucleus close in space is saturated by decoupling or by a selective 180° pulse. To understand this effect, we have to first consider the consequences of applying a second radio-frequency during an NMR experiment (decoupling).One

other key point to remember is that the effects of decoupling are almost instantaneous - once the decoupler is turned on coupling disappears on the order of fractions of a millisecond, when the decoupler is turned off, the coupling reappears on a similar time scale.

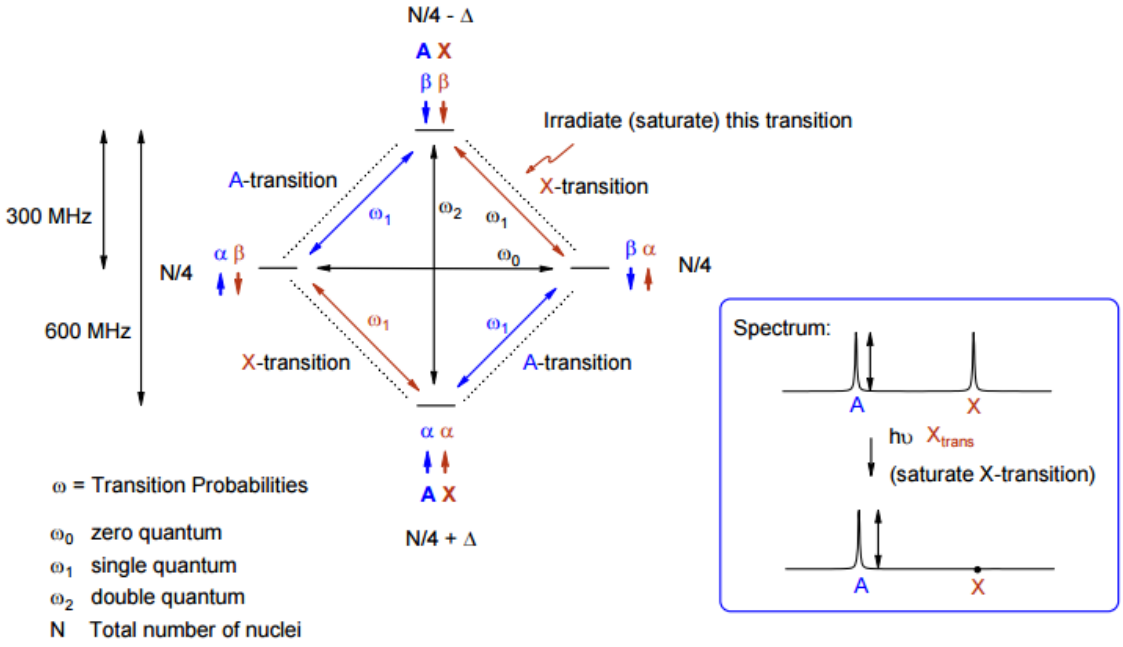

Figure 2.12: Nuclear Overhouser effect,schematic representation for two spin system showing trantions between population and the spectrum before and after saturation[15].

Now consider the situation when either the zero quantum or the double quantum processes are the only ones operative. In the zero quantum process, the dipolar interaction between A and X causes an A nucleus to undergo an $\alpha \rightarrow \beta$ transition when the X nucleus relaxes from $\beta \rightarrow \alpha$ i.e. $(\alpha\beta \rightarrow \beta\alpha)$. The net result is that as X returns to its normal population difference, it lowers the population difference for A. Thus, as the X intensity decreases, the A intensity decreases. If X is irradiated continuously then the signal for A will vanish (-ve NOE).This is a negative NOE.

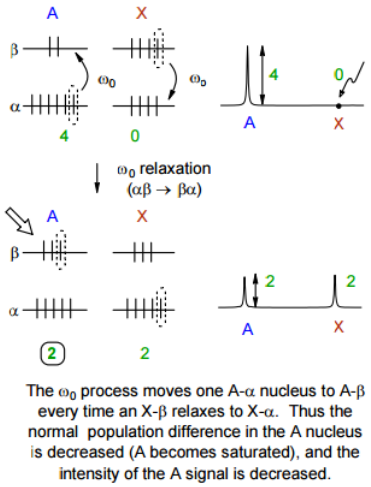

The ω_0 process moves one A-α nucleus to A-β every time an X-β relaxes to X-α. Thus the normal population difference in the A nucleus is decreased (A becomes saturated), and the intensity of the A signal is decreased.

Figure 2.13: schematic representation for -ve NOE[15].

For the double quantum process, each time an X nucleus relaxes from β to α state, and a nucleus also undergoes a β to α transition i.e. $(\beta\beta \rightarrow \alpha\alpha)$. This has the effect of increasing the population difference of A, i.e. an increase the area of A. This is a positive NOE. The phenomenon has sometimes been referred to as spin pumping - changing the population difference of X pumps A spins either from α to β or β to α.

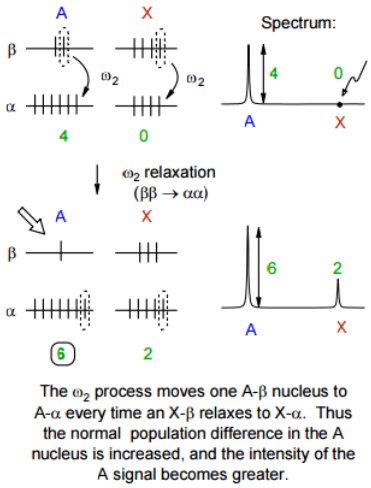

The ω_2 process moves one A-β nucleus to A-α every time an X-β relaxes to X-α. Thus the normal population difference in the A nucleus is increased, and the intensity of the A signal becomes greater.

Figure 2.14: schematic representation for +ve NOE[15].

2.1.5 Correlations and spectral density functions

As we have discussed earlier the local fields depend upon the orientation of the bond vectors. the mechanisms which influence these local fields are through either dipole-

dipole or Chemical Shift Anisotropy or both mostly. For now first we consider the backbone N-H bond vector with fixed orientation with respect to the molecular refrence frame in a protein. As the protein is free to do a brownian motion the N-H bond vector changes its positions when the protein tumbles in the solution with a overall correlation time τ_c. The changes in the orientation depends upon the rate of tumbling of the molecule. Faster the tumbling faster is the changes in the orientation of the bond vector. For large molecules or proteins which moves slow the changes in the bond vector orientation at time t and $t + \Delta$t do not differ too much and both the orientations are correlated in high degree. While for lighter proteins which are small

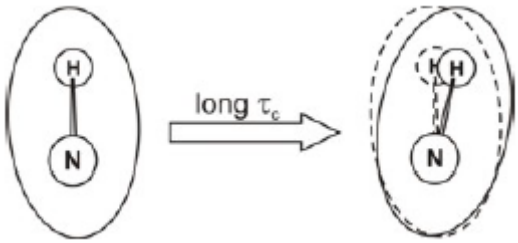

Figure 2.15: slow orientation change in large proteins[58].

in size the overall tumbling is quite faster ranges from milliseconds to microseconds, the bond vector changes its position rapidly so the orientation at time t and $t + \Delta t$ are very less correlated. So we can define a correlation function which decribes the loss of correlations after some time t.

For isotropic diffusion of spherical top correlation function is given by[58],

$$C_o(t) = \frac{1}{5} e^{-\frac{t}{\tau_c}}$$

Where τ_c is the overall rotational correlation time which can be calculated by hydrodynamic calculations or relaxation parameters and C_o is the correlation function for overall motion.

Now, the Fourier transformation of the correlation functions leads to spectral density function[52]. The spectral density functions play the main role in the model free for-

$$J(\omega) = \frac{2}{5} \frac{\tau_c}{1 + \omega^2 \tau_c^2}$$

malism. The Model free formalism is based on deriving the spectral density functions in terms of ordered parameters and correlation times.

The relaxation rates can be associated to spectral density function which gives us insight into the concept that how the relaxation parameters are associated in understanding model free formalism.

Longitudinal relaxation rate can be associated with spectral densities as[62, 52]

$$\begin{aligned} R_1 &= R_1^{\mathrm{DD}} + R_1^{\mathrm{CSA}} \\ &= \frac{d^2}{4}\left[J\left(\omega_{\mathrm{H}} - \omega_{\mathrm{X}}\right) + 3J\left(\omega_{\mathrm{X}}\right) + 6J\left(\omega_{\mathrm{H}} + \omega_{\mathrm{X}}\right)\right] + c^2 J\left(\omega_{\mathrm{X}}\right) \end{aligned}$$

Where d is the dipolar coupling constant and c is the CSA coupling constant which are defined as[14, 52],

$$d = \frac{\mu_0 \hbar \gamma_{\mathrm{H}} \gamma_{\mathrm{X}}}{4\pi r_{\mathrm{XH}}^3}$$

$$c = \frac{1}{\sqrt{3}} \omega_{\mathrm{X}} \Delta\sigma$$

where μ_0 is the permeability of the free space γ_H and γ_X are the gyromagnetic ratios of H^1 and the X spin (X is N^{15} here), respectively; r_{XH} is the XH bond length; ω_H and ω_X are the Larmor frequencies of the H^1 and X spins, respectively; and $\Delta\sigma$ is the chemical shift.

The transverse relaxation rate is given by[62, 52],

$$\begin{aligned} R_2 &= R_2^{\mathrm{DD}} + R_2^{\mathrm{CSA}} + R_{\mathrm{ex}} \\ &= \frac{d^2}{8}\left[4J\left(0\right) + J\left(\omega_{\mathrm{H}} - \omega_{\mathrm{X}}\right) + 3J\left(\omega_{\mathrm{X}}\right) + 6J\left(\omega_{\mathrm{H}}\right) + 6J\left(\omega_{\mathrm{H}} + \omega_{\mathrm{X}}\right)\right] \\ &\quad + \frac{c^2}{6}\left[4J\left(0\right) + 3J\left(\omega_{\mathrm{X}}\right)\right] + R_{\mathrm{ex}} \end{aligned}$$

R_{ex} is the chemical exchange contribution to R_2. Which can be calculated using multiple magnetic fields experiments. In contrast to the longitudinal relaxation rate

constant, R_2 increases monotonically with increasing τ_c.

Heteronuclear NOE in terms of spectral density functions[52, 58],

$$NOE = 1 + \frac{d^2}{4\,R_1}\frac{\gamma_X}{\gamma_H}\left[6\,J\left(\omega_H + \omega_X\right) - J\left(\omega_H - \omega_X\right)\right]$$

Where all the symbols used have their usual meaning. For pure dipoledipole interactions, the theoretical limits for extreme narrowing and slow tumbling are -3.93 and 0.78, respectively.

Chapter 3

Analysis of NMR relaxation data

3.1 Model-free analysis

NMR relaxation experiments provides wealth of information about molecular dynamics in macromolecules and fluids. There are many different software are available now a days to analyse protein dynamics. Since the preparation of input files as in accordance with the software in use are of different types and in many case are not easy to prepare in error free manner. And also creating and editing these file is also a tedious work which is prone to errors. To simplify many of these problem of data analysis the we used the FASTModelFree[8] a fully automated program to get the meaningful explanation of NMR relaxation data. In this program Model free approach for analysis of the data is used. Model free approach was introduced by G Lipari and A. Szabo in 1982[1] and further extended by G.M. Clore[17].

3.1.1 Theory

The relaxation data are most commonly analysed by fitting the model- free which have number of models containing a number of free parameters to the relaxation data or spectral density function[52, 59, 65]. Model free allows characterization of internal motions on time scales faster than the overall molecular tumbling utilizing the dependence of the longitudinal and transverse relaxation rates R_1 and R_2 and the heteronuclear NOE on the spectral density function $J(\omega)$.

Consider a $N^{15}H^1$ spin pair in a protein whose overall motion can be described by a single correlation time.The orientation of the bond vector is not fixed with respect to

a molecular frame of reference. Rather, it changes due to internal motions. Assuming that the overall and internal motions are independent, the total correlation function is given as[58]

$$C(t) = C_o(t)C_i(t)$$

Where the indices o and i refer to overall and internal motions, respectively. It should be emphasized that the independence of overall and internal motions is the fundamental assumption of the MF-approach. The overall correlation time as described earlier can be calculated by stokes law or using the longitudinal and transverse relaxation time and is given by

$$C_o(t) = \frac{1}{5}e^{-\frac{t}{\tau_c}}$$

Where, τ_c is the rotational correlation time of the molecule.
Fourier transformation of the correlation function gives us the spectral density function which is given as

$$J(\omega) = \frac{2}{5}\frac{\tau_c}{1+\omega^2\tau_c^2}$$

Since we are studying the protein, we know that not only the overall motions but also the internal motion study plays an important role to understand the protein fully. So when the protein tumbles in the liquid due to Brownian motion the bond vector changes it orientation in a correlation with the overall change in the orientation of the protein, considering that the bond vector has a fixed position with respect to the molecular frame. But since we know that the bond vector don't have a fix position with respect to the molecular frame. It is free to move within the protein and has an associated internal correlation time[58].

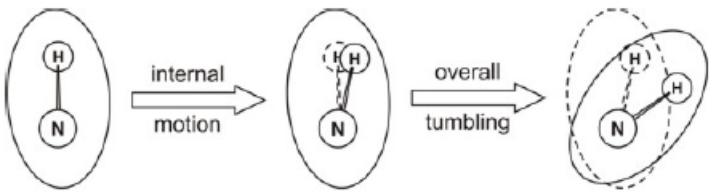

So as explained above a rough picture can be taken in our mind how the actual motion takes place. The bond vector changes its orientation due to both internal motions

and the overall motions. Depending upon the time scale of the motions the dynamics of the bond vector can be understood. But it gives us idea that along with the overall spectral density function we need to include the internal correlation functions which on Fourier transformation will give rise to internal spectral density function and the combined spectral density function to understand the full picture. So for the isotropic diffusion the internal correlation function can be expressed as[1, 52]

$$C_i(t) = S^2 + (1-S^2)\, e^{-\frac{t}{\tau_i}}$$

Where τ_i is the correlation time and S^2 is the squared order parameter of the internal motion.

Parameter S^2 describes the spatial restriction of the motion with two limiting values (0,1). Now the total correlation function is given as[58]

$$C(t) = \frac{1}{5} e^{-\frac{t}{\tau_c}} \cdot \left[S^2 + \left(1 - S^2\right) e^{-\frac{t}{\tau_i}} \right]$$

With the basic assumption of the model free that internal motions and the overall motions are independent which is not actually true sometimes and puts a restriction to extant of understandings. Now the Fourier transformation of the correlation function will give rise to the spectral density function which is equal to[1, 18]

$$J(\omega) = \frac{2}{5}\left[\frac{\tau_c}{1+\omega^2\tau_c^2} + \frac{(1-S^2)\tau'}{1+\omega^2\tau'^2} \right]$$

Where τ' is related to the rotational and internal correlation times according to the relation,

$$\frac{1}{\tau'} = \frac{1}{\tau_c} + \frac{1}{\tau_i}$$

Now, using the Lipari-Szabo formalism by parametrizing the correlation function of the internal motions as[58, 1]

$$C_i(t) = C_f(t) \cdot C_s(t) = S^2 + \left(1 - S_f^2\right) e^{-\frac{t}{\tau_f}} + \left(S_f^2 - S^2\right) e^{-\frac{t}{\tau_s}}$$

Since the internal motions can be divided into two parts as suggested by Lipari and

Szabo having two different time scale of the motions which is fast and the slow with reference to the overall correlation time of the protein. In above equation, f and s subscripts are used for fast and the slow motions and the Sf is defined to be the order parameter for fast internal motion.

So using this definition in total correlation function and Fourier transforming this we get the final form of the spectral density function for isotropic diffusion tensor and given by[27, 30]

$$J(\omega) = \frac{2}{5}\left[\frac{S^2\tau_c}{1+\omega^2\tau_c^2} + \frac{(1-S_f^2)\,\tau_f'}{1+\omega^2\tau_f'^2} + \frac{(S_f^2-S^2)\,\tau_s'}{1+\omega^2\tau_s'^2}\right]$$

where k = f or s and $\tau_k^{'}$ is defined as

$$\tau_k^{'} = \frac{\tau_k\tau_c}{\tau_k+\tau_c}$$

This was the result for the spectral density function for isotropic diffusion tensor. If we consider the axially symmetric diffusion tensor for the protein the model free spectral density function is given by[17]

$$J(\omega) = \frac{2}{5}\sum_{j=1}^{3} A_j\left[\frac{S^2\tau_j}{1+\omega^2\tau_j^2} + \frac{(1-S_f^2)\,\tau_f'}{1+\omega^2\tau_f'^2} + \frac{(S_f^2-S^2)\,\tau_s'}{1+\omega^2\tau_s'^2}\right]$$

Which will give rise to the same result which we have derived above. if we consider the isotropic tensor then[52],

$$J(\omega) = \frac{S^2\tau_m}{1+\omega^2{\tau_m}^2} + \frac{(1-S^2)\tau}{1+\omega^2\tau^2}$$

Because for isotropic diffusion[52],

$$D_{\|} = D_{\perp} = D\sum A_j = 1,\ and\ \tau_m = \tau_j = (1/6D)$$

with

$$\tau = (1/\tau_m + 1/\tau_e)^{-1}$$

Here τ_m is same overall rotational correlation time, τ_m is used here because in many literatures the the overall correlation time in case of protein is represented

$$J(\omega) = \frac{2}{5} S_f^2 \sum_{j=0}^{2} A_j \left[\frac{S_s^2 \tau_j}{1 + \omega^2 \tau_j^2} + \frac{(1 - S_s^2)\tau_j'}{1 + \omega^2 \tau_j'^2} \right]$$

by[52] τ_m which is same as τ_c. A more complex expression is needed if we consider a fully anisotropic diffusion tensor where

$$(D_{xx} \neq D_{yy} \neq D_{zz})$$

3.1.2 Model free parameters

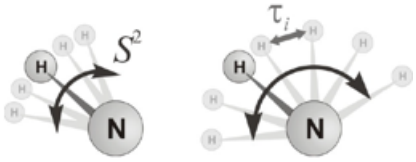

Figure 3.1: Schematic representation of order parameter and internal rotational time of N-H bond vector[58].

Considering the N-H bond vector in the protein, the bond vector can have the various degree of freedom depending upon the environment and can have the dynamics accordingly. To understand the model free analysis we first need to understand the model free parameters which can be derived by various model fitting by model free approach and gives us different information about the dynamics of the proteins.
S^2 **:** S^2 describes the spatial restriction of the motion that is how freely the bond vector can move. If the value of the order parameter is 1 then motion of given residue is highly restricted and if it is 0 then motion is unrestricted. It is basically the measure of equilibrium distribution of different orientation of bond vector $\mu(t)$ in molecular reference frame and mathematically given by[17, 1],

$$S^2 = (4\pi/5) \sum_{m=-2}^{2} |\langle Y_2^m(\theta,\phi)\rangle|^2$$

${Y_2}^m(\theta, \phi)$ are spherical harmonic functions of the orientations of $\mu(t)$ in a molecular reference frame, defined by (θ, ϕ). The ensemble average is defined by In which[1]

$$\langle Y_2^m(\theta,\phi)\rangle = \int_0^{2\pi} \int_0^{\pi} p(\theta,\phi)\, Y_2^m(\theta,\phi)\, \sin\theta \, d\theta \, d\phi$$

probability $P(\theta, \Phi)$ is the probability of finding the N-H bond vector in (θ, ϕ) and is given by, After simplifying if we consider the model in which bond vector have a

$$p(\theta,\phi) = \exp[-\beta W(\theta,\phi)]/\int_0^{2\pi}\int_0^{\pi}\exp[-\beta W(\theta,\phi)]\sin\theta\, d\theta\, d\phi$$

restricted diffusion in a cone then S^2 is given as[1],

$$S^2 = [\cos\theta_0\,(1+\cos\theta_0)/2]^2$$

Where θ_o is cone semi-angle and the motion is characterised by this angle.
While if we consider the model in which bond vector have a diffusion with restricted parabolic potential[29] on the surface of a cone then S2 is given as[48],

$$S^2 = 1 - 3\sin^2\theta\,\{\cos^2\theta\,(1-\exp[-\sigma_f^2]) + 0.25\sin^2\theta\,(1-\exp[-4\sigma_f^2])\}$$

in which θ is the (fixed) angle between $\mu(t)$ and the director axis for the motion and σ_f is the standard deviation of the fluctuation in the azimuthal angle.
For small fluctuation[52],

$$S^2 = 1 - 3\sin^2\theta\sigma_f^2$$

For large fluctuation[52],

$$S^2 = P_2[\cos\theta]^2$$

τ_i- It is internal correlation time of corresponding residues. It is the time taken by the bond vector to move by one radian.
R_{ex}- It gives the relaxation dispersion and is related with the residues undergoing chemical exchange.
But we will not talk about it often in our analysis rather it also gives us many information because for the accuracy and less error possibility we need to have multiple magnetic field data to analyse the chemical exchange.

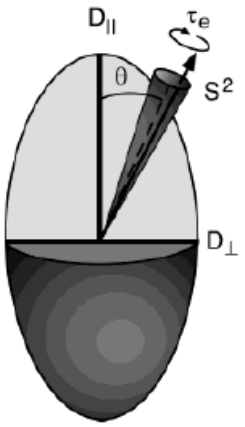

Model-free parameters for axially symmetric diffusion tensor[52, 1, 8]. The diffusion constants are $D_{\parallel}$ for diffusion around the symmetry axis of the diffusion tensor and $D_{\perp}$ for diffusion around the two orthogonal axes. The equilibrium position of the I-S bond vector is oriented at an angle θ with respect to the symmetry axis of the diffusion tensor. Local dynamics of the bond vector are depicted as stochastic motions within the shaded cone and are characterized by the order parameter S^2, and the effective internal correlation time.

3.1.3 Definition of Model

In order to extract the motional parameters described in the previous section, the experimental data have to be fitted against the equations defining the relaxation rates using the appropriate forms of the spectral density , or versions of these modified to account for axially symmetric or anisotropic tumbling. Fitting the experimental data using the spectral density function of the extended Lipari-Szabo model for isotropic tumbling requires at most six parameters. In most cases, only three experimental parameters are available: the longitudinal and transverse relaxation rates and the hetero-nuclear NOE. Hence, a maximum of four parameters can be extracted from this data.

Model 1 and 3 Model 1 is the most simple model of all and requires only one parameter: the squared order parameter S^2. For this model[58], the internal motions are assumed to be very fast, with the correlation time for the internal motion $\tau_i << \tau_c$, and the spectral density function is given by

$$J(\omega) = \frac{2}{5}\frac{\tau_c}{1+\omega^2\tau_c^2}$$

In the case of chemical exchange as an additional source of relaxation, R_{ex} is introduced as second fit parameter in model 3.

Model 2 and 4[1] Model 2 is sometimes referred to as the classical Lipari- Szabo. Here, τ_i is relaxation active and the spectral density function is defined by Again, R_{ex}

$$J(\omega) = \frac{2}{5}\left[\frac{\tau_c}{1+\omega^2\tau_c^2} + \frac{(1-S^2)\tau^{'}}{1+\omega^2\tau^{'2}}\right]$$

is introduced in the case of chemical exchange to yield model 4.

Model 5[58] The extended Lipari-Szabo model includes a fast and a slow internal motion with their internal correlation times differing by at least one order of magnitude; the spectral density function is given by[1, 58] The motions can be described by

$$J(\omega) = \frac{2}{5}\left[\frac{S^2\tau_c}{1+\omega^2\tau_c^2} + \frac{(1-S_f^2)\,\tau_f'}{1+\omega^2\tau_f'^2} + \frac{(S_f^2-S^2)\,\tau_s'}{1+\omega^2\tau_s'^2}\right]$$

diffusion- or wobbing-in-a-cone as fast and a two-site jump as slow motion.

Table with different Models and parameters for fitting relaxation data to the model-free spectral densitiy functions. Now the overview of the fitting of the models by[58]

Model	fitted parameter(s)
1	S^2
2	S^2, $\tau_i = \tau_f$
3	S^2, R_{ex}
4	S^2, $\tau_i = \tau_f$, R_{ex}
5	S_f^2, S^2, $\tau_i = \tau_s$

model- free approach as a brief summery in Model-free analysis of NMR relaxation data R_1, R_2 and NOE acquired at single magnetic field proposed by Mandel et al.

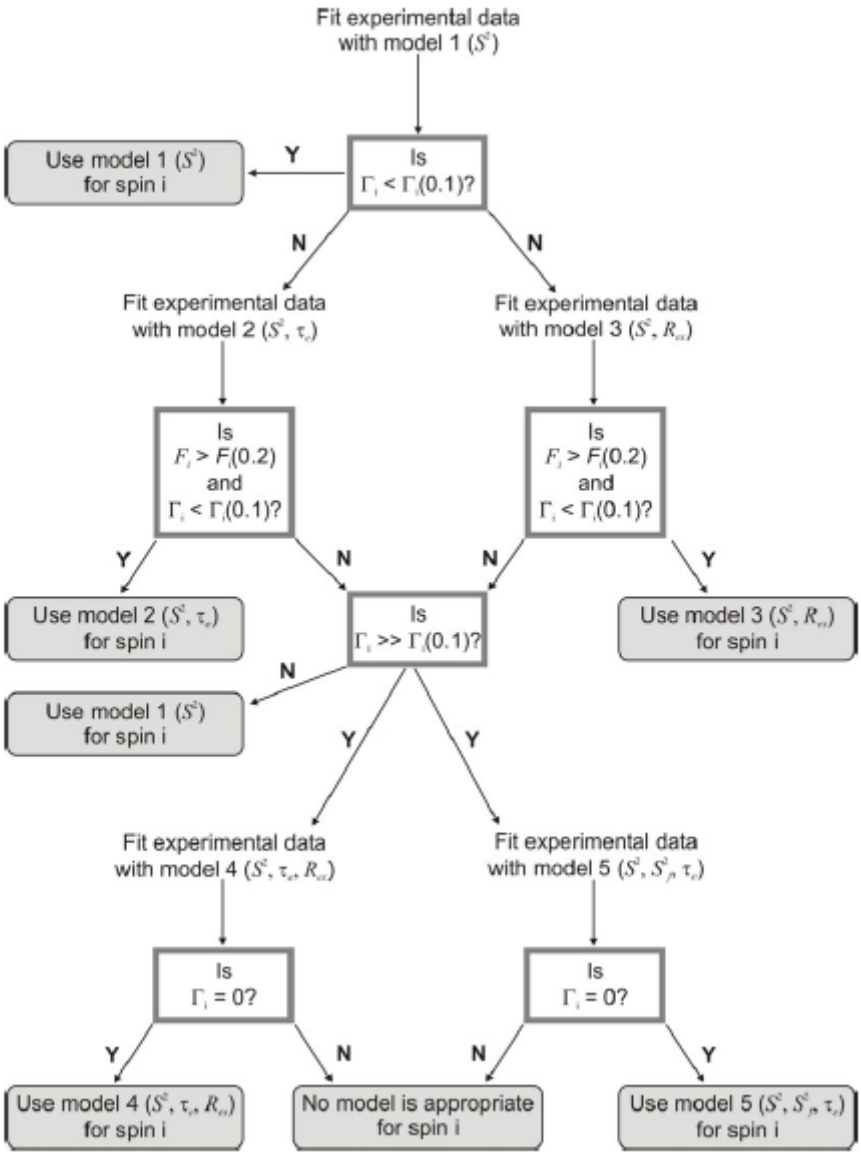
Fit experimental data with model 1 (S^2)
Is $\Gamma_i < \Gamma_i(0.1)$?
Y
Use model 1 (S^2) for spin i
N
N
Fit experimental data with model 2 (S^2, τ_e)
Fit experimental data with model 3 (S^2, R_{ex})
Is $F_i > F_i(0.2)$ and $\Gamma_i < \Gamma_i(0.1)$?
Is $F_i > F_i(0.2)$ and $\Gamma_i < \Gamma_i(0.1)$?
Y
N
N
Y
Use model 2 (S^2, τ_e) for spin i
Is $\Gamma_i >> \Gamma_i(0.1)$?
Use model 3 (S^2, R_{ex}) for spin i
N
Use model 1 (S^2) for spin i
Y
Y
Fit experimental data with model 4 (S^2, τ_e, R_{ex})
Fit experimental data with model 5 (S^2, S^2_f, τ_e)
Is $\Gamma_i = 0$?
Is $\Gamma_i = 0$?
Y
N
N
Y
Use model 4 (S^2, τ_e, R_{ex}) for spin i
No model is appropriate for spin i
Use model 5 (S^2, S^2_f, τ_e) for spin i

Chapter 4

Results,Discussion and Conclusion

4.1 Results

4.1.1 Relaxation parameters for ubiquitin

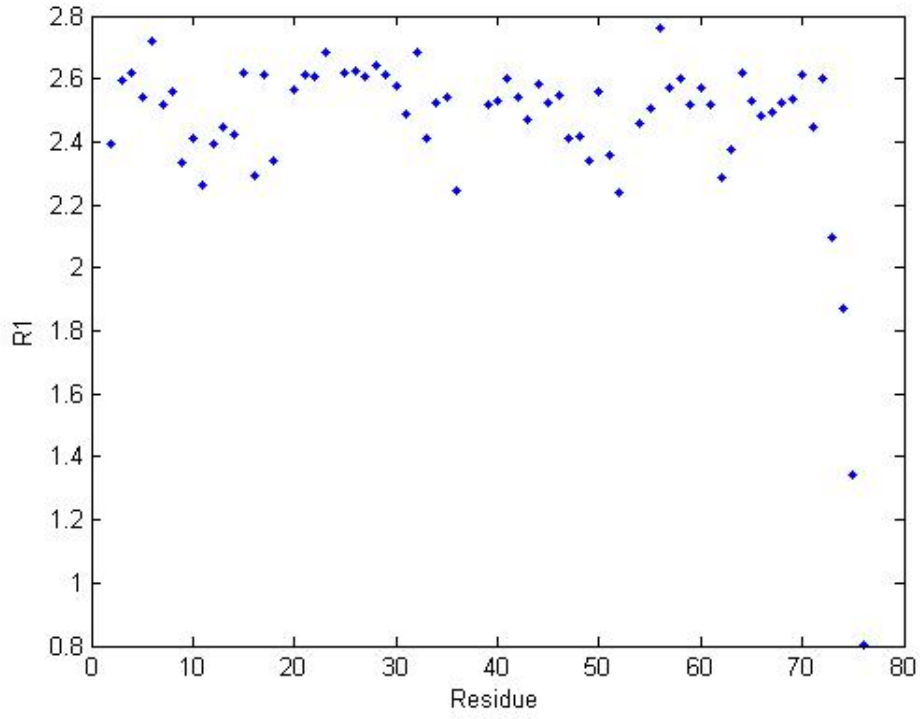

Figure 4.1: Plot longitudinal relaxation with residue. Ubiquitin has 76 residues. X-axis is residue no. while y-axis represents longitudinal relaxation rate (1/s).

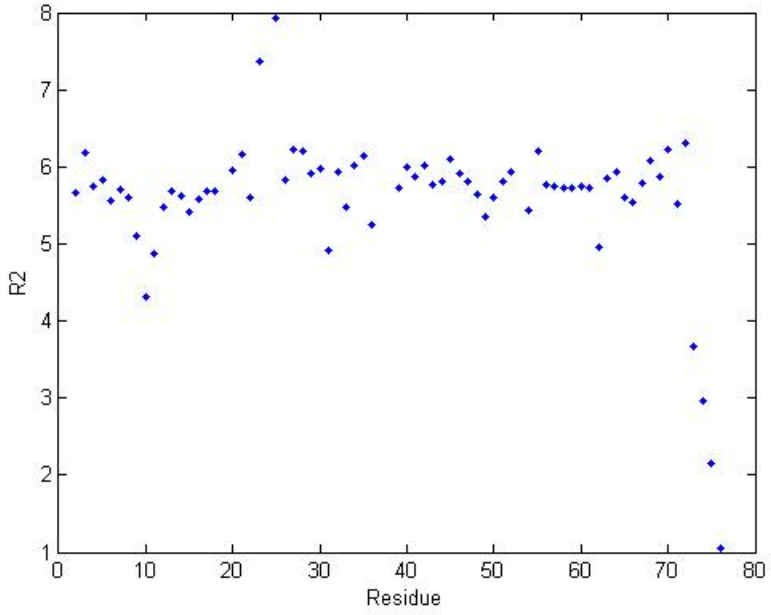

Figure 4.2: Plot trnasverse relaxation with residue. X-axis is residue no. while y-axis represents transverse relaxation rate (1/s).

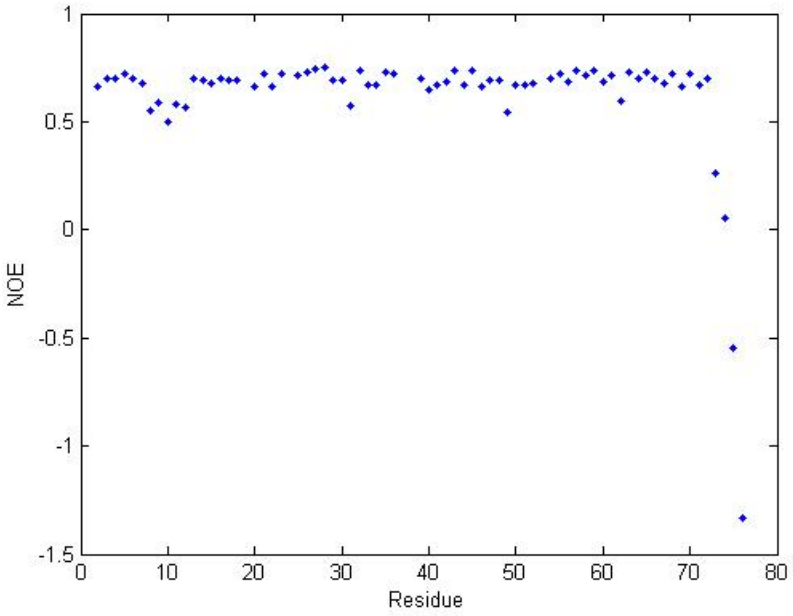

Figure 4.3: Plot of Heteronuclear NOE with residue. X-axis is residue no. while y-axis represents NOE values.

4.1.2 Model-free parameters

For isotropic diffusion tensor[8]

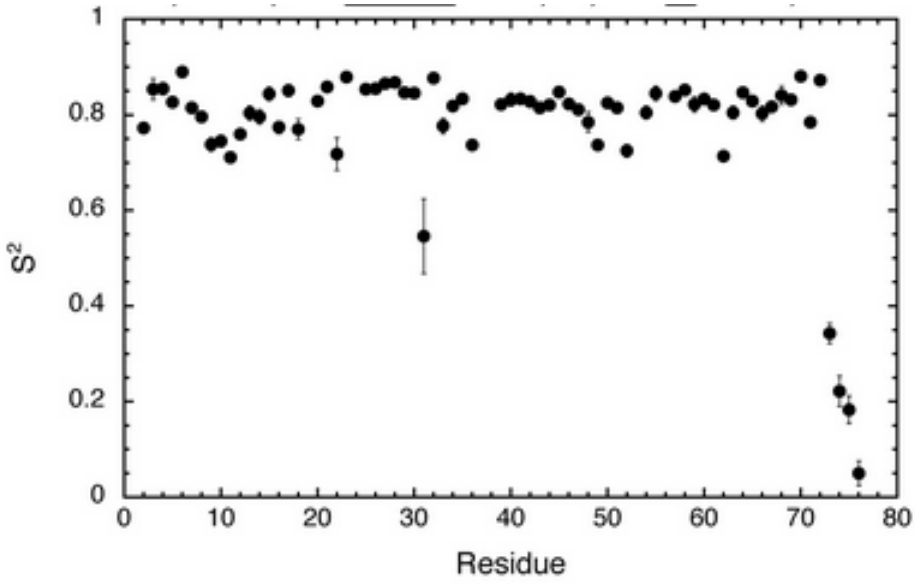

For axially symmetric diffusion tensor:

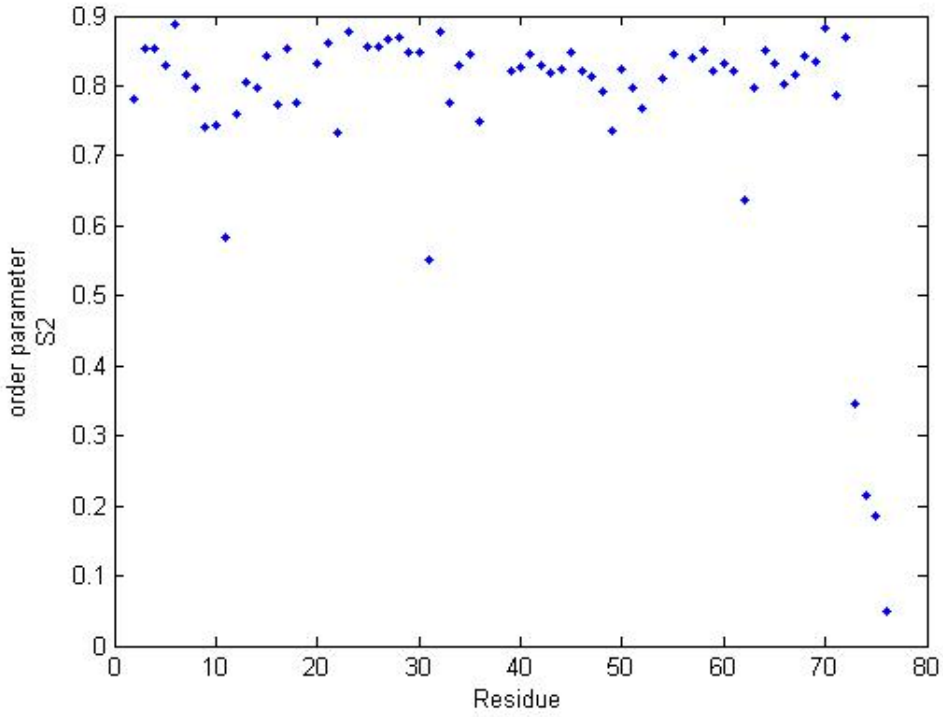

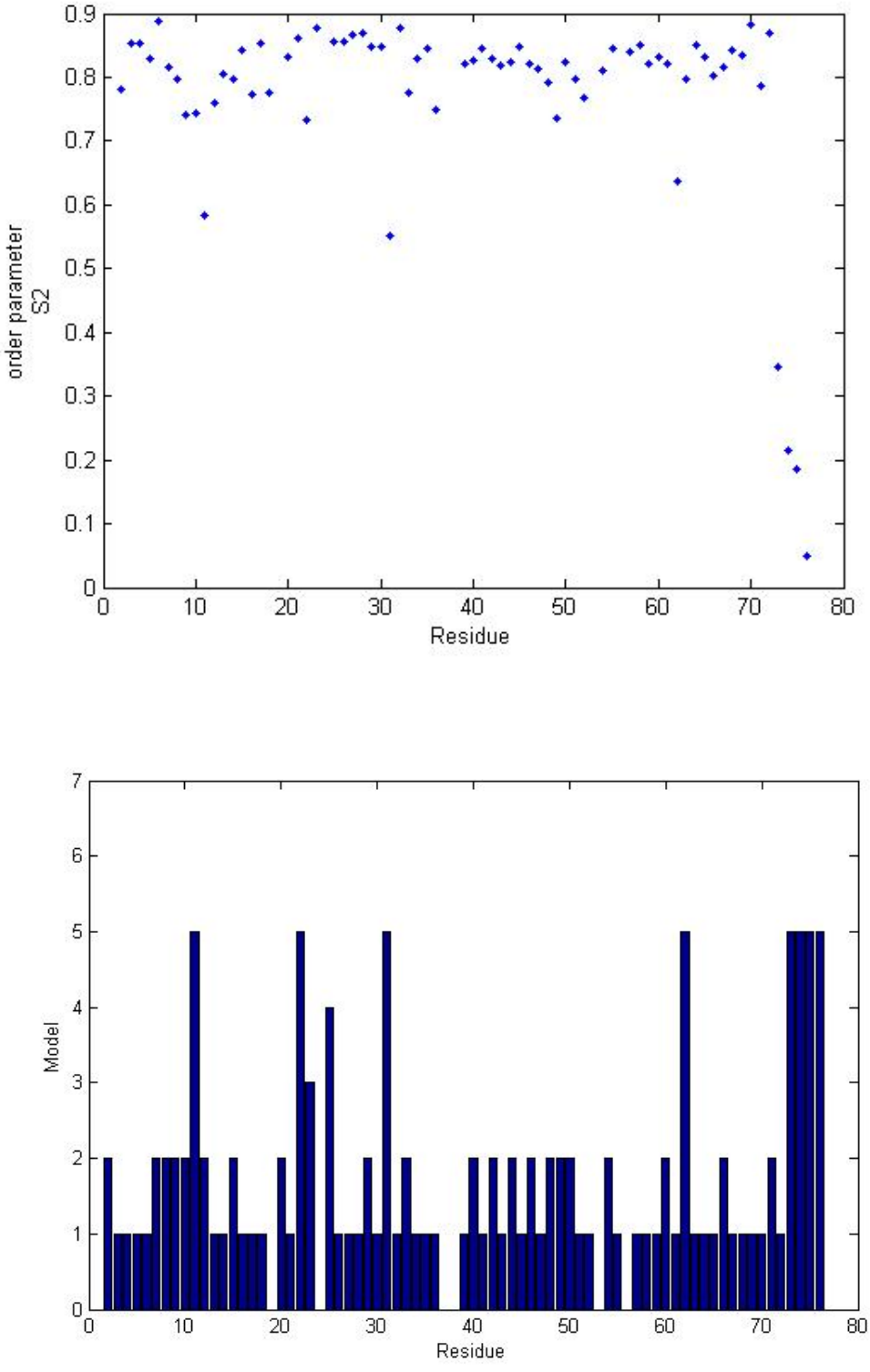

Figure 4.4: A direct comparison for the residue specific information by Model fitting and the order-parameter with residue number in Ubiquitin.

Model free parameters information from the generated ubiquitin.log file generated from model free analysis :

Residues: 69

Tensor:

tm = 4.272

Dratio = 1.189

Theta = 30.381

Phi = 49.612

Model 1 spins:

3 4 5 6 13 14 16 17 18 21 26 27 28

30 32 34 35 36 39 41 43 45 47 51 52

55 57 58 59 61 63 64 65 67 68 69 70 72

Model 2 spins:

2 7 8 9 10 12 15 20 29 33 40 42 44 46 48

49 50 54 60 66 71

Model 3 spins:

23

Model 4 spins:

25

Model 5 spins:

11 22 31 62 73 74 75 76

Unassigned spins:

56

Delta tm: 0.0000 Converged? YES

Delta Dratio: 0.0000 Converged? YES

Delta Theta: 0.0020 Converged? YES

Delta Phi: 0.0040 Converged? YES

Model free parameters for RNase using axially diffusion tensor:

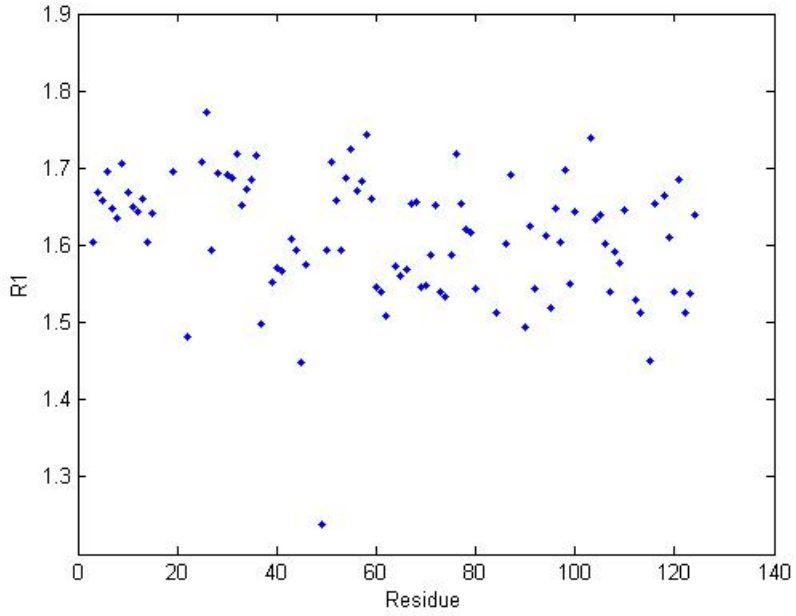

Figure 4.5: Plot longitudenal relaxation with residue. X-axis is residue no. while y-axis represents longitudinal relaxation rate (1/s) for RNase.

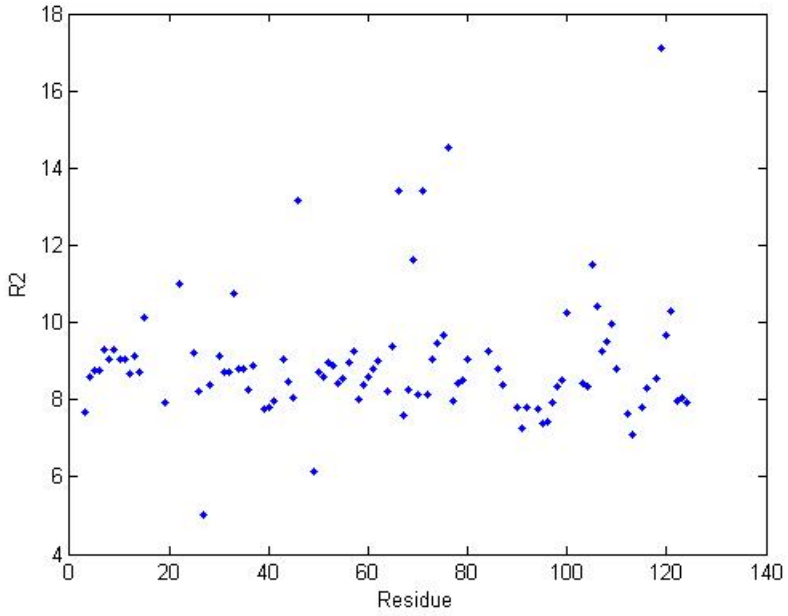

Figure 4.6: Plot transverse relaxation with residue. X-axis is residue no. while y-axis represents transverse relaxation rate (1/s) for RNase.

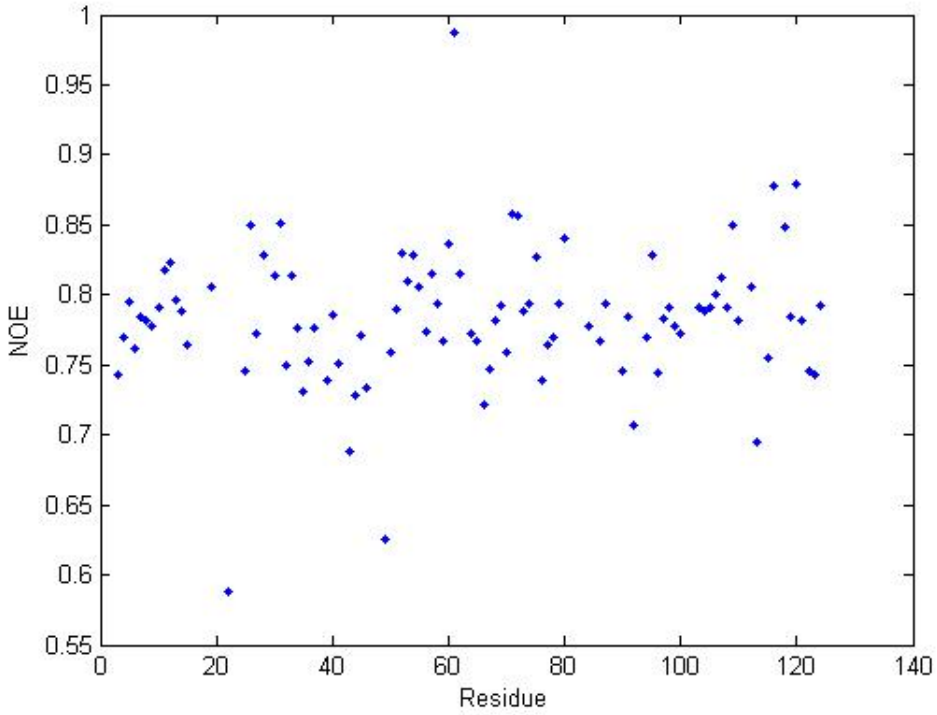

Figure 4.7: Plot of Heteronuclear NOE with residue. X-axis is residue no. while y-axis represents NOE values for RNase.

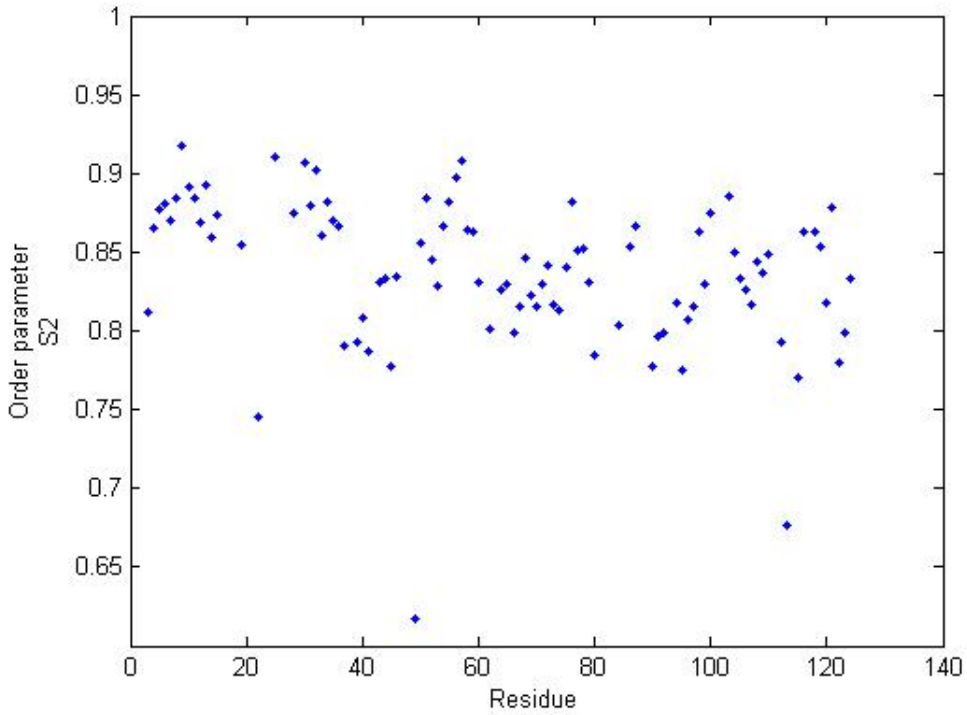

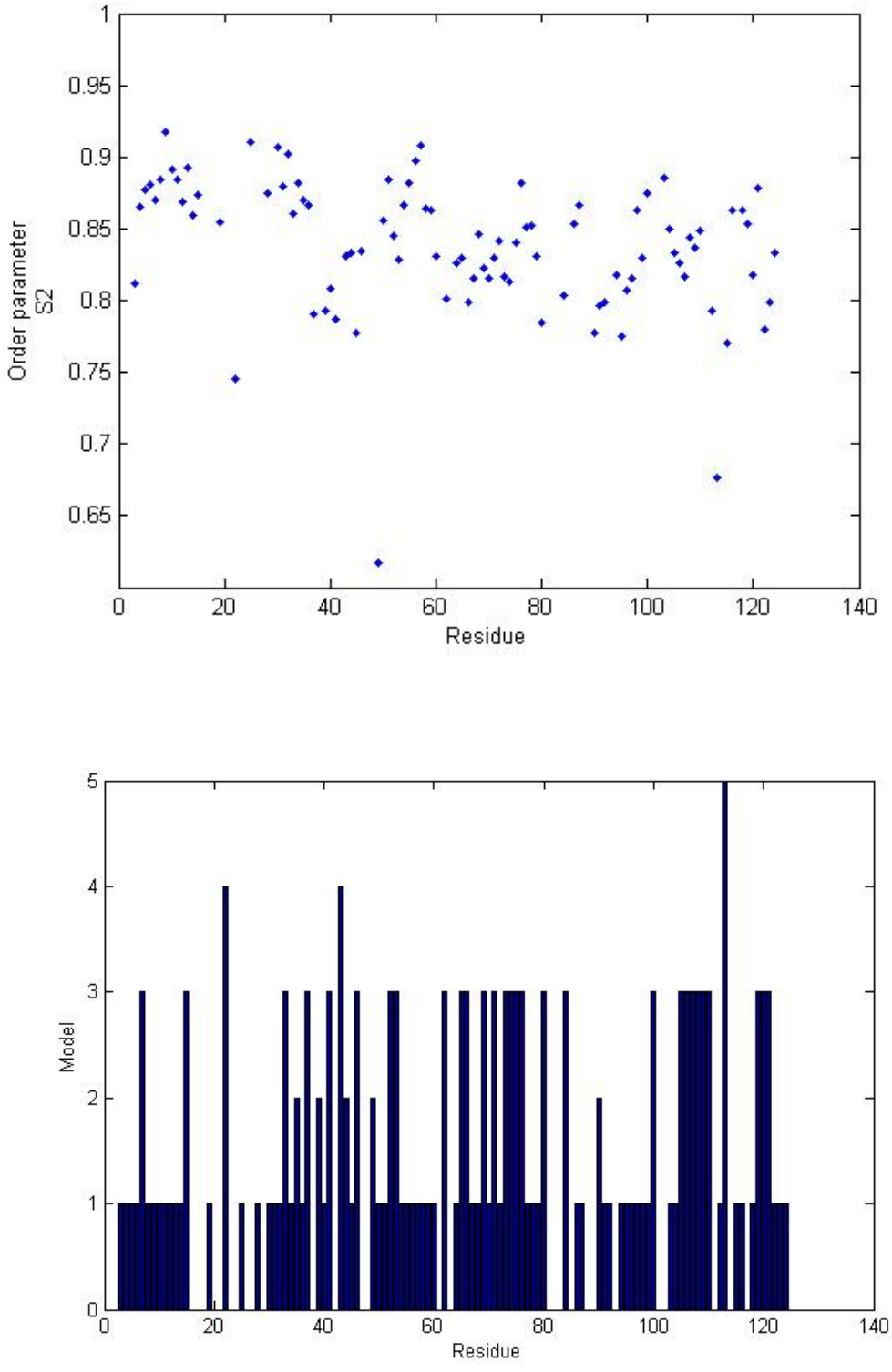

Figure 4.8: A direct comparison for the residue specific information by Model fitting and the order-parameter with residue number in RNase.

Model free parameters information from the generated RNase.log file generated from model free analysis :

Residues: 94

Diffusion Tensor:

tm = 6.463

Dratio = 0.844

Theta = 15.570

Phi = 146.230

Model 1 spins:

3 4 5 6 8 9 10 11 12 13 14 19 25 28 30 31 32 34 36 40 45

50 51 54 55 56 57 58 59 60 64 67 68 70 72 77 78 79 86 87

91 92 94 95 96 97 98 99 103 104 112 115 116 118 122 123 124

Model 2 spins:

35 39 44 49 90

Model 3 spins:

7 15 33 37 41 46 52 53 62 65 66 69 71 73 74 75 76 80 84 100

105 106 107 108 109 110 119 120 121

Model 4 spins:

22 43

Model 5 spins:

113

Unassigned spins:

26 27 61

Delta tm: 0.0000 Converged? YES

Delta Dratio: 0.0000 Converged? YES

Delta Theta: 0.0010 Converged? YES

Delta Phi: 0.0010 Converged? YES

4.2 Conclusion

Model-free analysis is a very good method to study the dynamics of the proteins but has very high limitations for other biomolecule like RNA and DNA due to various

reasons. Model free gives us various parameters which are very useful in understanding dynamics of proteins. For example the parameters Dratio, theta, phi derived from the analysis gives us the information about the optimised diffusion tensor and also provides us the improved PDB structure file combining structure and dynamics in a single frame. The order parameter provides us degree to which a residue can move freely and each residue can be probed specifically with very less limitations by using model free analysis. The parameters derived using the axially diffusion tensor have advantage as compare to the isotropic diffusion which is almost a crude assumption in case of proteins. But for the proteins like ubiquitin and RNase the results do not very much and the information can be carried with both. The errors in the parameters derived from model free analysis are very small and are order of third decimal place and even the residue with high errors or which does not fit any model can be discarded. But for the better dynamics study of proteins one can try a fully anisotropic diffusion tensor in future which have advantage over axially symmetric diffusion tensor.

Bibliography

[1] Lipari, G.; Szabo, *J. Am. Chem. Soc.* **104**, 1982

[2] Atkinson, R. A.; Kieffer, B.; Prog, *Nucl. Magn. Reson. Spectrosc.* **44**, 2008

[3] Wand, A. J., *Nat. Struct. Biol.* **8**, 2001

[4] Jackson, E. S., *Folding Des.* **3**, 1998

[5] Fersht, A, *Enzyme Structure and Mechanism* **45**, 1985

[6] Frueh, D., . *Nucl. Magn. Reson. Spectrosc.* **41**, 2002

[7] Palmer, A. G, *Annu. Rev. Biophys. Biomol. Struct* **30**, 2001

[8] Cole, R.; Loria, J. P, *J. Biomol. NMR* **26**, 2003

[9] Cavanagh, J.; Fairbrother, W. J.; Palmer, A. G.; Skelton, N. J., *Protein NMR Spectroscopy: Principles and practice; Academic Press: San Diego* **cA**, 1996

[10] Kay, L. E.; Torchia, D. A.; Bax, A, *Biochemistry* **28**, 1978

[11] Millet, O.; Muhandiram, D. R.; Skrynnikov, N. R.; Kay, L. E., *J. Am. Chem. Soc.* **124**, 2002

[12] Skrynnikov, N. R.; Millet, O.; Kay, L. E., *J. Am. Chem. Soc.* **124**, 2002

[13] Wang, T.; Cai, S.; Zuiderweg, E. R. P., *J. Am. Chem. Soc* **125**, 2003

[14] Abragam, A., *Clarendon Press: Oxford* **U.K.**, 1961

[15] Hans J. Reich, *https://www.chem.wisc.edu/areas/reich/nmr/08-tech-02-noe.htm* , 2017

[16] Rowan, McCammon, Sykes, , *J. Am. Chem. Soc.* **96**, 1974

[17] Clore, G. M.; Szabo, A.; Bax, A.; Kay, L. E.; Driscoll, P. C.; Gronenborn, , *A. M. J. Am. Chem. Soc.* **112**, 1990

[18] Mayo, K. H.; Daragan, V. A.; Idiyatullin, D.; Nesmelova, I, *J. Magn. Reson.* **146**, 2000

[19] Bru schweiler, R.; Case, D. A, *Phys. Rev. Lett.* **72**, 1994

[20] Led, J. J.; Gesmar, H.; Abildgaard, F., *Methods Enzymol* **176**, 1989

[21] LeMaster, D. M., *J. Am. Chem. Soc.* **121**, 1999

[22] Lienin, S. F.; Bremi, T.; Brutscher, B.; Bru schweiler, R.; Ernst, R. R., *J. Am. Chem. Soc.* **120**, 1998

[23] Meirovitch, E.; Shapiro, Y. E.; Liang, Z.; Freed, J. H., *J. Phys. Chem. B* **107**, 2003

[24] Tugarinov, V.; Liang, Z.; Shapiro, Y. E.; Freed, J. H.; Meirovitch, E., *J. Am. Chem. Soc.* **123**, 2001

[25] Buevich, A. V.; Baum, J., *J. Am. Chem. Soc.* **121**, 1999

[26] Ochsenbein, F.; Neumann, J.-M.; Guittet, E.; Van Heijenoort, C., *Protein Sci.* **11**, 2002

[27] Halle, B.; Wennerstrom, H., *J. Chem. Phys.* **75**, 1981

[28] Schurr, J. M.; Babcock, H. P.; Fujimoto, B. S., *J. Magn. Reson.* **105**, 1995

[29]) Bremi, T.; Bru schweiler, R., *J. Am. Chem. Soc.* 1977

[30] Bru schweiler, R.; Wright, P. E., *J. Am. Chem. Soc.* **116**, 1994

[31] Geoffrey Bodenhousen, *https://www.youtube.com/watch?v=SUkTmyzslaM* 2015

[32] Geoffrey Bodenhousen, *https://www.youtube.com/watch?v=bs4sKiStzvw* 2015

[33] Markley, J. L.; Horsley, W. J.; Klein, M. P, *J. Chem. Phys.* **55**, 1995

[34] Shaka, A. J.; Barker, P. B.; Freeman, R., *J. Magn. Reson.* **64**, 1985

[35] Meiboom, S.; Gill, D., *Rev. Sci. Instrum.* **58**, 1958

[36] Carr, H. Y.; Purcell, E. M, *Phys. Rev.* **94**, 1954

[37] Logan, T. M.; Olejniczak, E. T.; Xu, R. X.; Fesik, S. W., *J. Biomol. NMR* **3**, 1993

[38] Grzesiek, S.; Bax, A., *J. Magn. Reson. B* **102**, 1993

[39] Morris, G. A.; Freeman, R, *J. Am. Chem. Soc.* **101**, 1999

[40]] Farrow, N. A.; Muhandiram, R.; Singer, A. U.; Pascal, S. M.; Kay, C. M.; Gish, G.; Shoelson, S. E.; Pawson, T.; Forman-Kay, J. D.; Kay, L. E.; , *Biochemistry* **33**, 1994

[41] Goldman, M., *J. Magn. Reson.* **60**, 1984

[42] Kay, L. E.; Nicholson, L. K.; Delaglio, F.; Bax, A.; Torchia, D. A, *J. Magn. Reson.* **72**, 1992

[43] Boyd, J.; Hommel, U.; Campbell, I. D., *Chem. Phys. Lett.* **1990**, 85

[44] Kay, L. E.; Nicholson, L. K.; Delaglio, F.; Bax, A.; Torchia, D. A, ,

[45] Levitt, M. H, *Spin Dynamics Basics of Nuclear Magnetic Resonance;Wiley* **New York**, 2001

[46] Pang, Y.; Buck, M.; Zuiderweg, E. R. P., *Biochemistry* **41**, 2002

[47] Fischer, M. W. F.; Majumdar, A.; Zuiderweg, E. R. P., *Prog. Nucl. Magn. Reson. Spectrosc.* **33**, 1998

[48] Palmer, A. G.; Rance, M.; Wright, P. E., *J. Am. Chem. Soc.* **113**, 1991

[49] Mandel, A. M.; Akke, M.; Palmer, A. G., *J. Mol. Biol.* **246**, 1995

[50] Cole, R.; Loria, J. P, *J. Biomol. NMR* **26**, 2003

[51] Palmer, A. G., *Annu. Rev. Biophys. Biomol. Struct.* **30**, 2001

[52] Palmer, A. G, *Chem. Rev. 2004* **104**, 2004

[53] Roger Cole and J. Patrick Loria, *Journal of Biomolecular NMR* **26**, 2003

[54] Vugmeyster, L.; Kroenke, C. D.; Picart, F.; Palmer, A. G.; Raleigh, D. P, *J. Am. Chem. Soc.* **122**, 2003

[55] Dyson, H. J.; Wright, P. E., *Annu. Rev. Phys. Chem.* **47**, 1996

[56] Jackson, E. S., *Folding Des.* **3**, 1998

[57] J. Aramini, *NESG targets* **table of rotational correlation time values** , 2010

[58] Markus Heller, *Protein Dynamics of ADT and KdpBN* **3**, 2004

[59] Anil kumar, P.K.Madhu, *Protein Dynamics of ADT and KdpBN* **37**, 2000

[60] Arthur.G.Palmer, *NYSBC* **Model-free analysis of 15N relaxation data** , 2006

[61] L E Kay, D A Torchia, A Bax, *Biochemistry* **23**, 1989

[62] Cavanagh J., Fairbrother W.J., Palmer, A.G, Rance M., Skelton N.J, *Protein NMR Spectroscopy: Principles and Practice, Elsevier* **P21** , 2007

[63] NSEG wiki, *http://mediatum.ub.tum.de/doc/601356/601356.pdf* **Rotational correlation time**, 2011

[64] J.W. Emsley, J.Feeney,*progress in NMR spectroscopy* **Vol-14**, 1980

[65] James Keeler, *NMR spectroscopy by James keeler* **edition second**, 2010

[66] WIKIMEDIA COMMONS *http://commons.wikimedia.org/wiki/file:T2relaxation.svg*, 2010